

Applications of Genetic Optimization at ALS & Electron Beam Diagnostics using Compton Scattering Technique

Changchun Sun

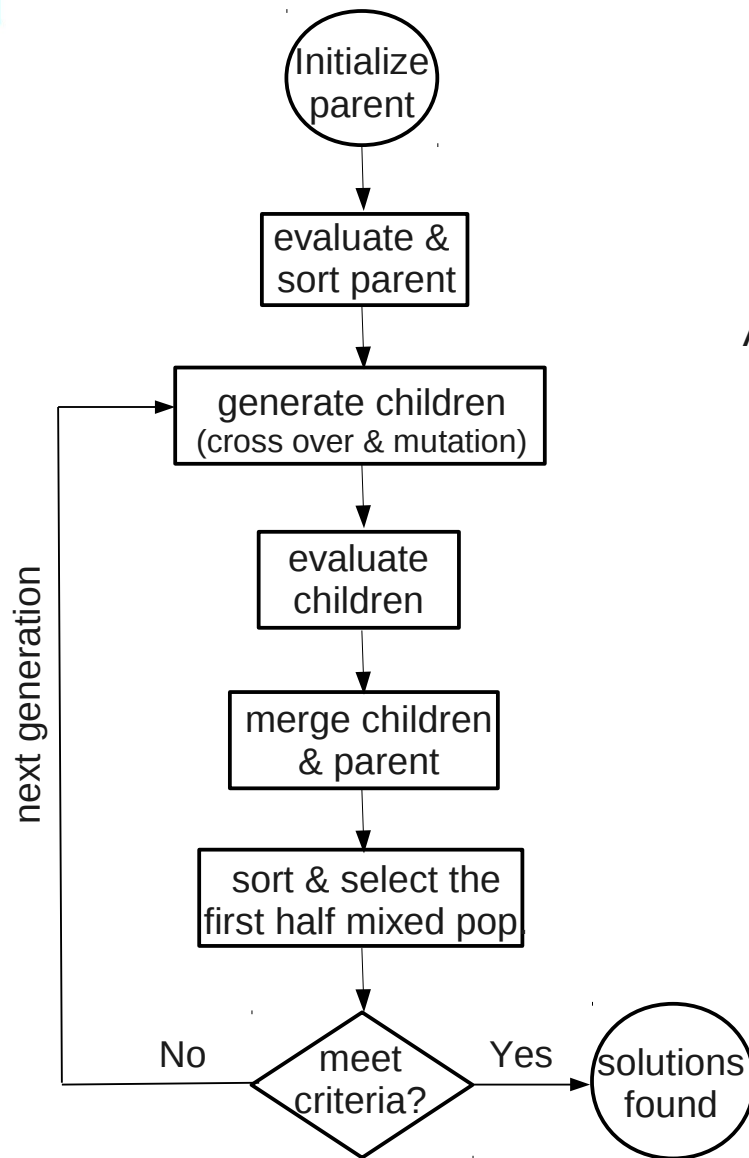
Advanced Light Source (ALS)
Lawrence Berkeley National Laboratory

Outline of the Talk

- Multi-Objective Genetic Algorithms (MOGAs)
- Applications at ALS
 - Low emittance lattice design and optimization for ALS upgrades
 - Curved superconducting combined-function magnet design
 - Spreader design and optimization for NGLS
- Electron beam diagnostics using Compton scattering technique

Genetic Algorithm (GA)

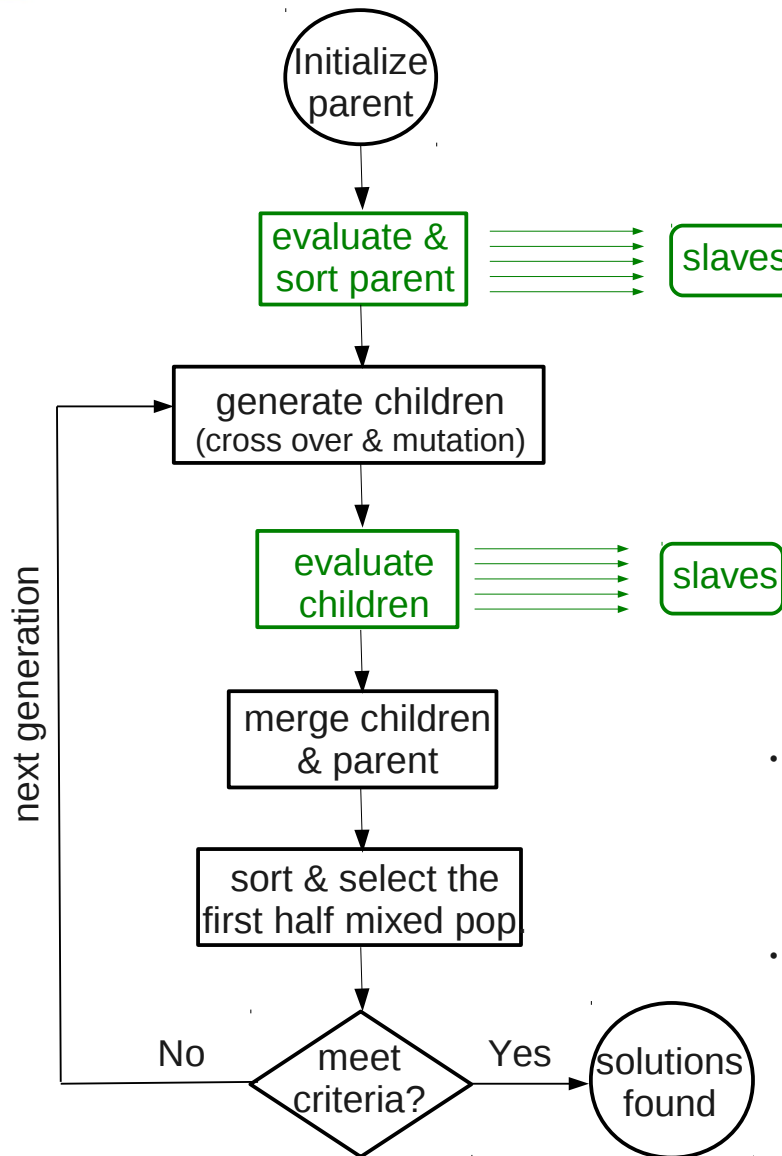
- Genetic Algorithm (GA) has been around 40 years. It was invented by John Holland and presented in his book "Adaption in Natural and Artificial Systems" from 1975.
- GA is a method to generate optimum solutions using techniques inspired by natural evolution, such as inheritance, mutation, selection and crossover.
- It is very suitable to solve complex multi-objective, multi-variable optimization problems. It can quickly scan a vast solution set with trade-offs among the objectives.
- GAs have been widely used in many fields. However, it was only introduced to accelerator community several years ago, and quickly attracts a lot of interest.



A Pseudo code:

- 1: Randomly generate the first generation
- 2: Evaluate the first generation
- 3: Sort the first generation
- 4: **Repeat**
- 5: select parent to generate child (cross over)
- 6: mutate child
- 7: evaluate child
- 8: merge the parent and child
- 9: sort the mixed population
- 10: select the first half of the mixed populations
- 11: **Until** reach maximum generation

- For some optimization problems, usually, a large number of populations and generations are needed, and evaluation of objectives are often very time consuming.
- Cluster-based Master-Slave computing strategy
 - *Master CPU performs genetic operations, such as cross over, mutation and selection, and distributes tasks to slave processors.*
 - *Slave CPUs evaluate the objective of problem and send the results back to master.*
- Each slave performs their tasks independently, and there are no communication between them.

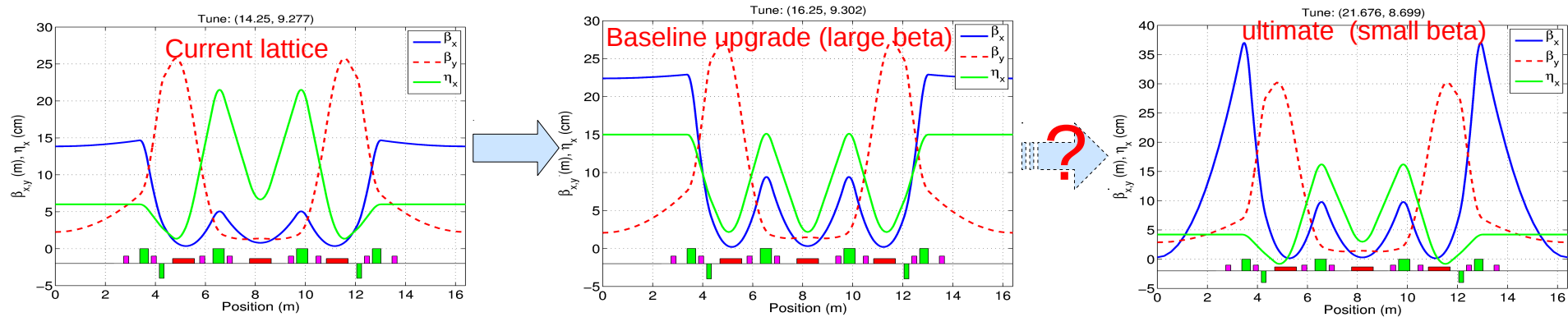


- At ALS, we have developed a flexible and reliable Genetic Optimization tool using our own cluster (328 CPUs).
- We have successfully applied this optimization tool to different project.

Outline of the Talk

- Multi-Objective Genetic Algorithms (MOGA)
- Applications at ALS
 - Low emittance lattice design and optimization for ALS upgrade
 - Curved superconducting combined-function magnet design
 - Spreader design and optimization for NGLS
- Electron beam diagnostics using Compton scattering technique

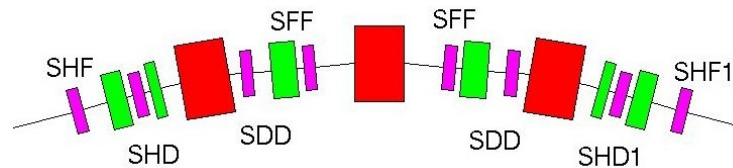
- The ALS is one of the earliest 3rd generation light sources, commissioned in 1993.
- The project of the low emittance upgrade began in 2009. After the upgrade finish, the brightness will be increased by 3 factors.



- The baseline upgrade lattice has a large-beta and dispersion function at the center of straight, and it doesn't provide ultimate insertion device brightness.
- **Challenges for ultimate low beta lattice:**
 1. Small dynamic aperture ----> need to be optimized
 2. Not compatible with traditional injection---> high and low beta lattice

Dynamic Aperture Optimization

- Genetic algorithm is used to optimize the dynamic aperture of the low-beta lattice
- **6 parameters:** (2 chromatic + 4 harmonic sextupoles)

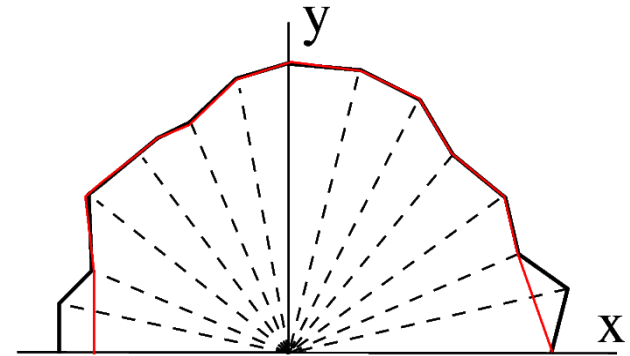


The chromatic sextupole strength are given by chromaticities fitting

- **Objectives:**
 - Dynamic aperture area, which is commonly used or
 - Total diffusion rates, newly proposed.

- **Dynamic aperture area** [M. Borland, *Elegant V 23.1*]

- **Dynamic aperture area** [M. Borland, *Elegant V 23.1*]
 - 21 line, and 11 steps for each line
 - 4 interval splitting to refine the boundary
 - 512 turns
 - Boundary is clipped to avoid the island

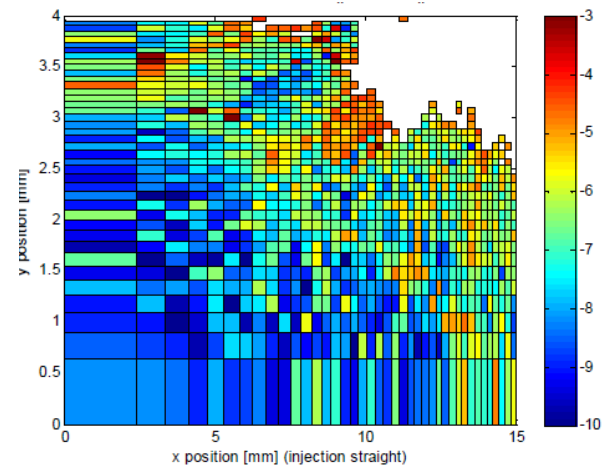


- **Total diffusion rate** [C. Steier and W. Wan, IPAC 2010]

- **Total diffusion rate** [C. Steier and W. Wan, IPAC 2010]
 - Frequency Map Analysis
 - 21 by 21 non-uniform grid search
 - 512 turns for each grid.
 - Diffusion rate is calculated according to

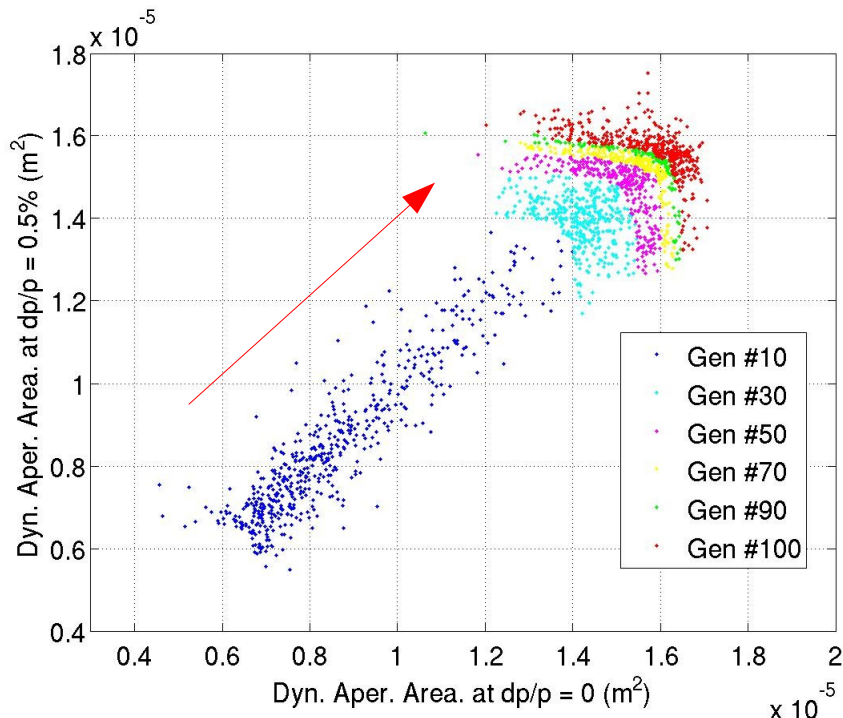
$$d = \log \left(\frac{\sqrt{(v_{x,1} - v_{x,2})^2 + (v_{y,1} - v_{y,2})^2}}{N} \right)$$

- **Total diffusion rate** [C. Steier and W. Wan, IPAC 2010]
 - Diffusion rate is assigned to -3 for lost particle
 - Boundary is clipped to avoid the island

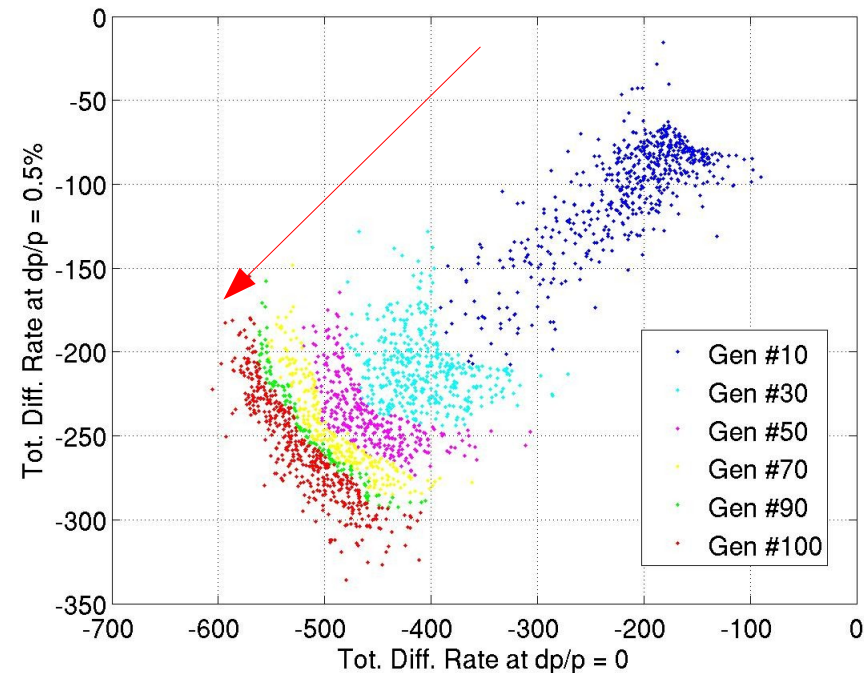


Objectives at Different Generation

The lattice errors: 0.03% quad field gradient and 0.05% coupling.

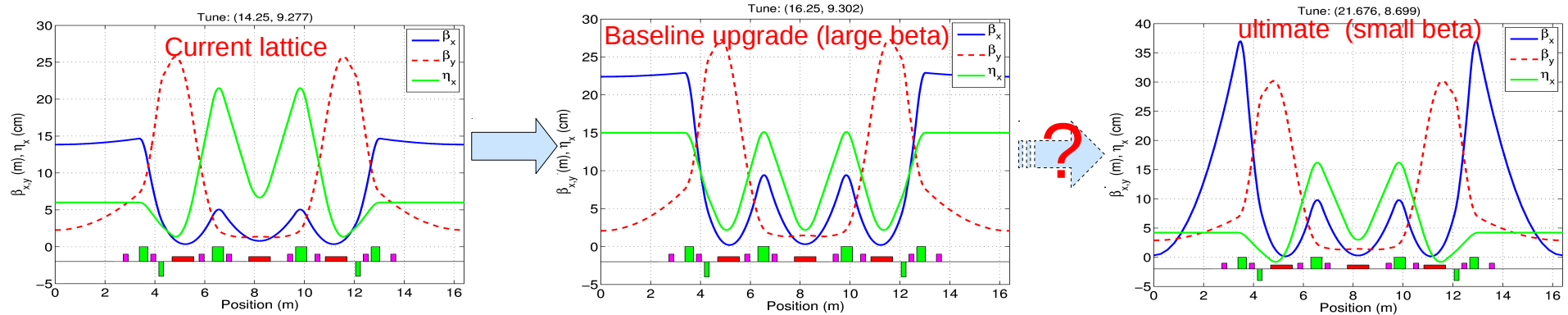


Dynamics aperture area



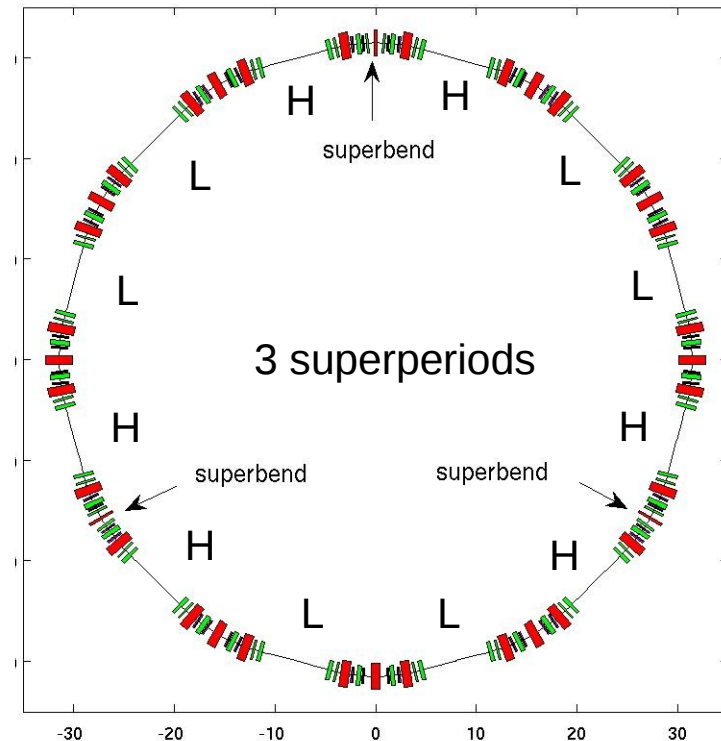
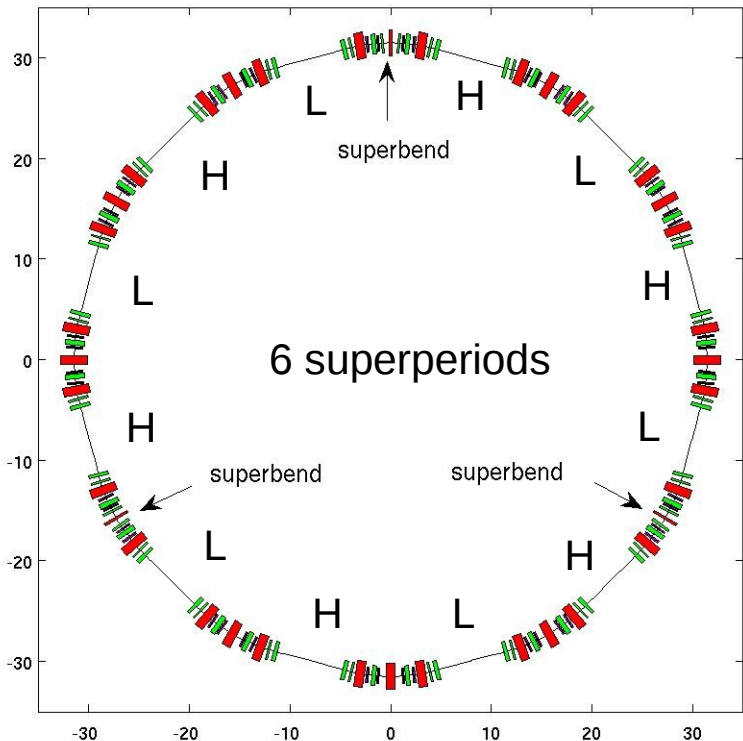
Total Diffusion Rate

- The ALS is one of the earliest 3rd generation light sources, commissioned in 1993.
- The project of ALS low emittance upgrade began in 2009. After the upgrade finish, the brightness will be increased by 3 factors.



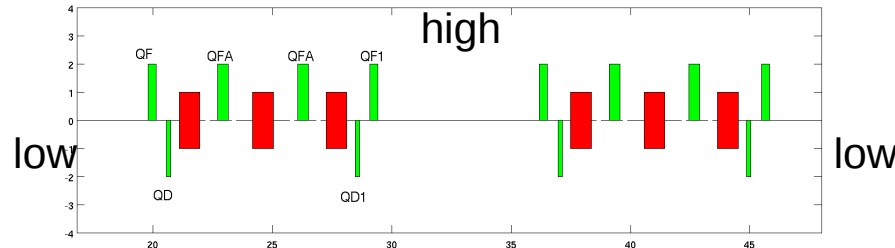
- The baseline upgrade lattice has a large-beta and dispersion function at the center of straight, and it doesn't provide ultimate insertion device brightness.
- Challenges for ultimate low beta lattice:
 - Small Dynamic aperture ----> need to be optimized
 - Not compatible with traditional injection---> high and low beta lattice

Two Options for High-Low Beta Lattice

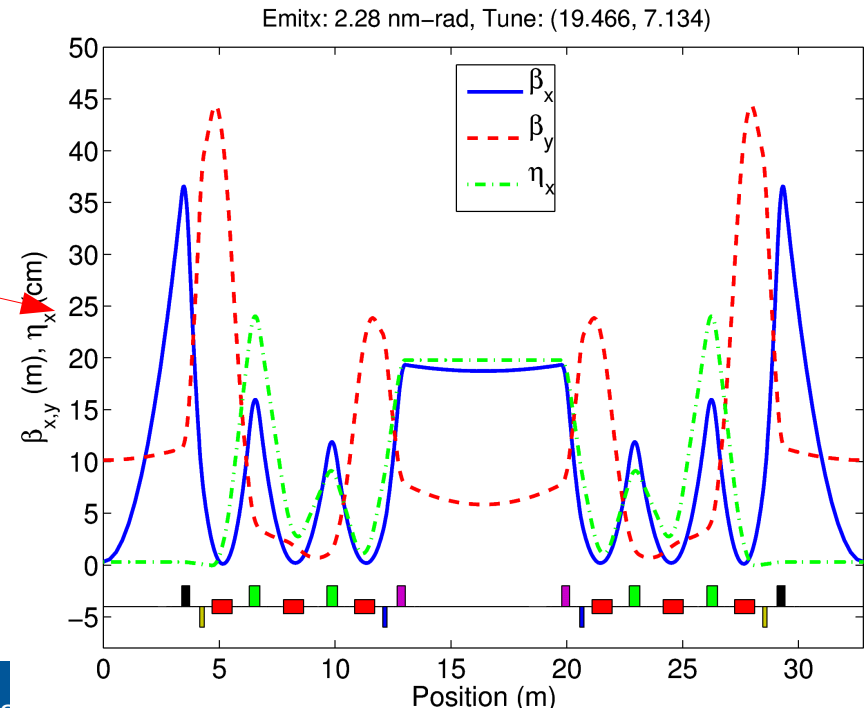
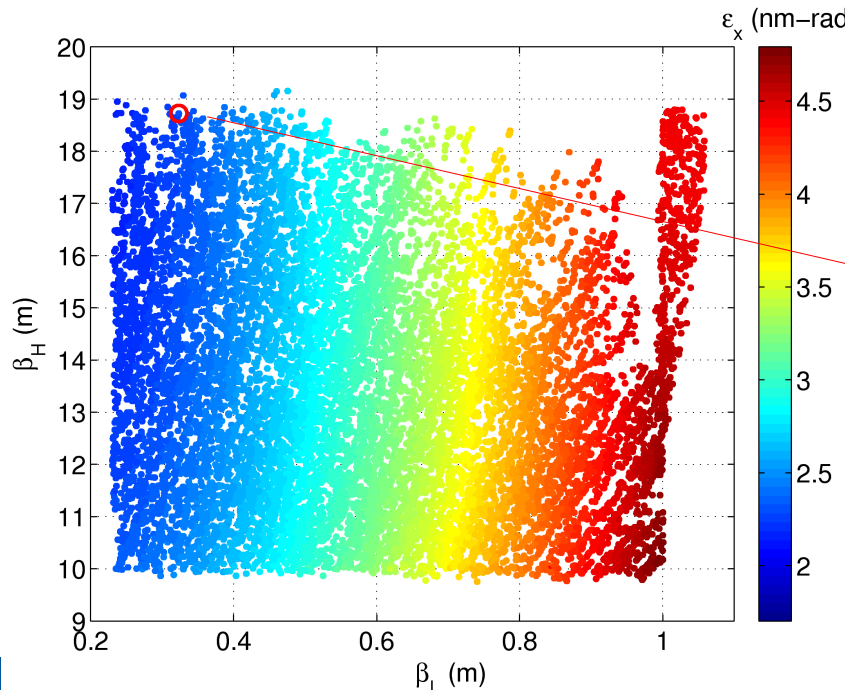


Genetic Algorithm (GA) is used to design these high-low beta lattices

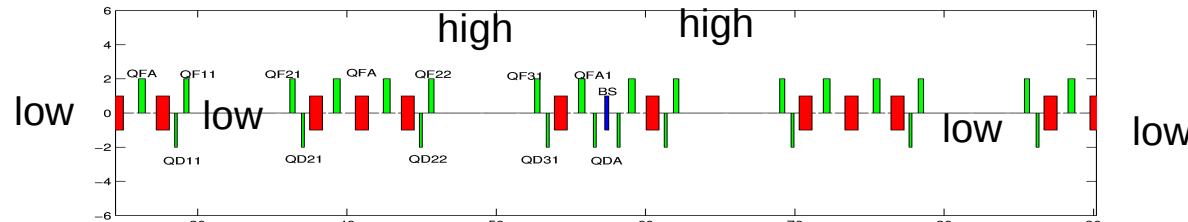
6 Superperiods High-Low Beta Lattice



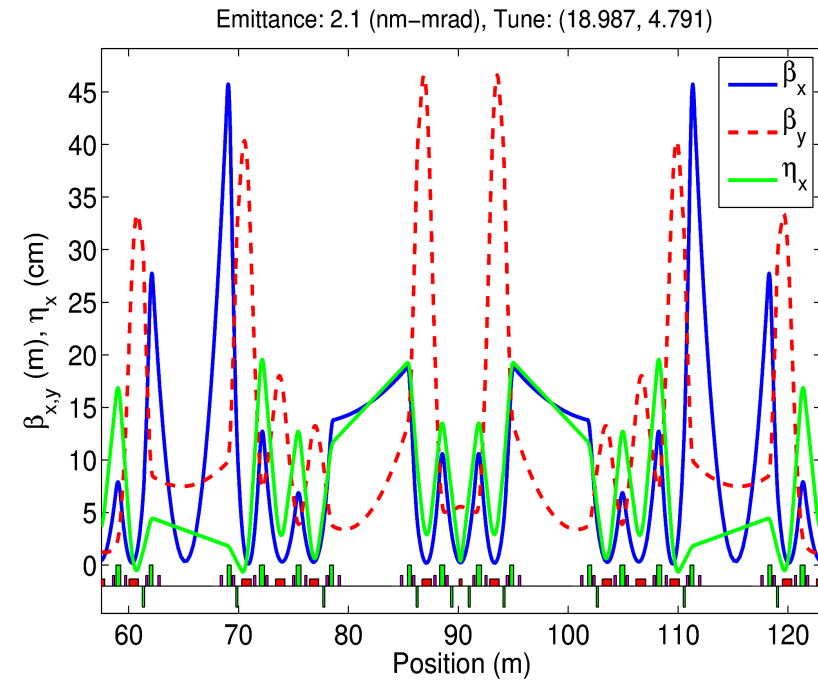
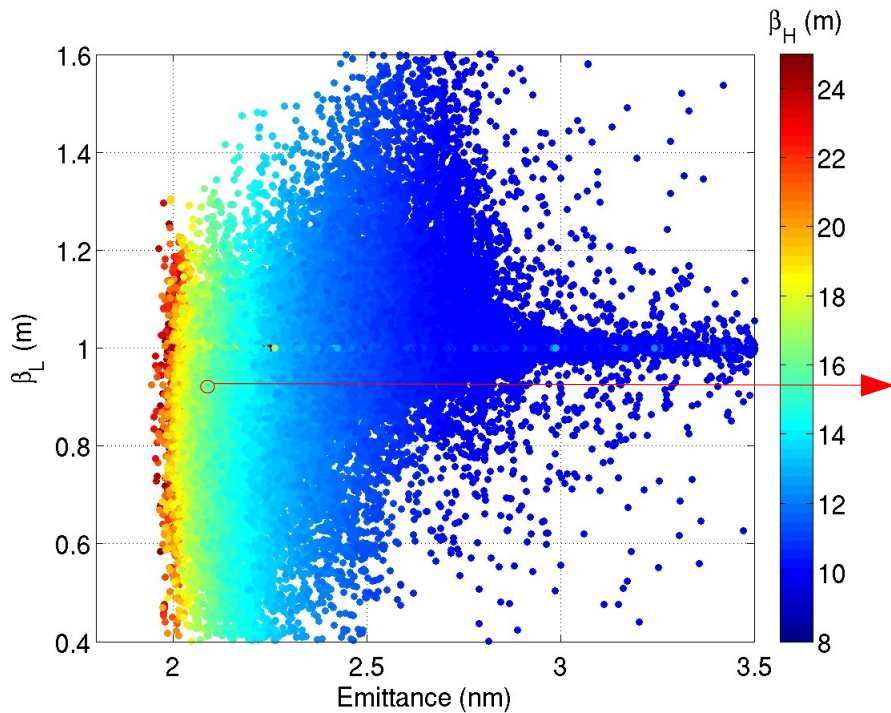
- **5 parameters:** QF, QD, QFA, QF1, QD1
- **7 constraints:** stability, positive partition number, maximum beta and dispersion functions
- **3 objectives:** $|\beta_L - 1|$, $|\beta_H - 10|$ and ε_x



3 Superperiods L-H-H-L Beta Lattice



- **11 parameters:** QFA, QD11, QF11, QF21, QD21, QD22, QF22, QF31, QD31, QFA1, QDA
- **7 constraints:** stability, positive partition number, maximum beta and dispersion functions
- **3 objectives:** $|\beta_L - 1|$, $|\beta_H - 10|$ and ε_x

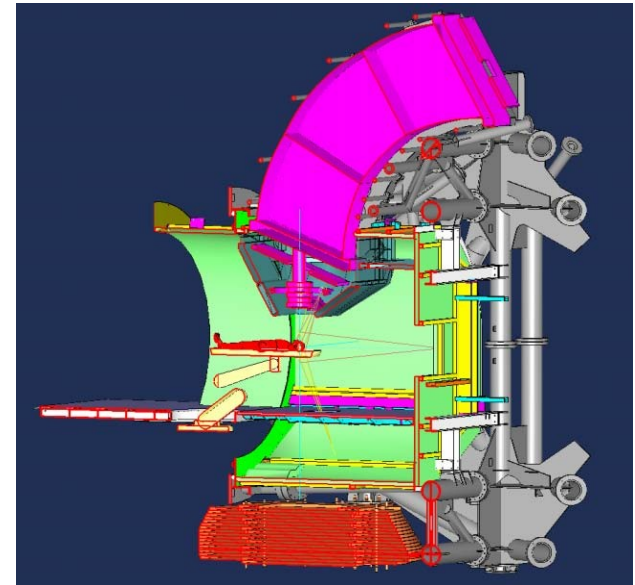
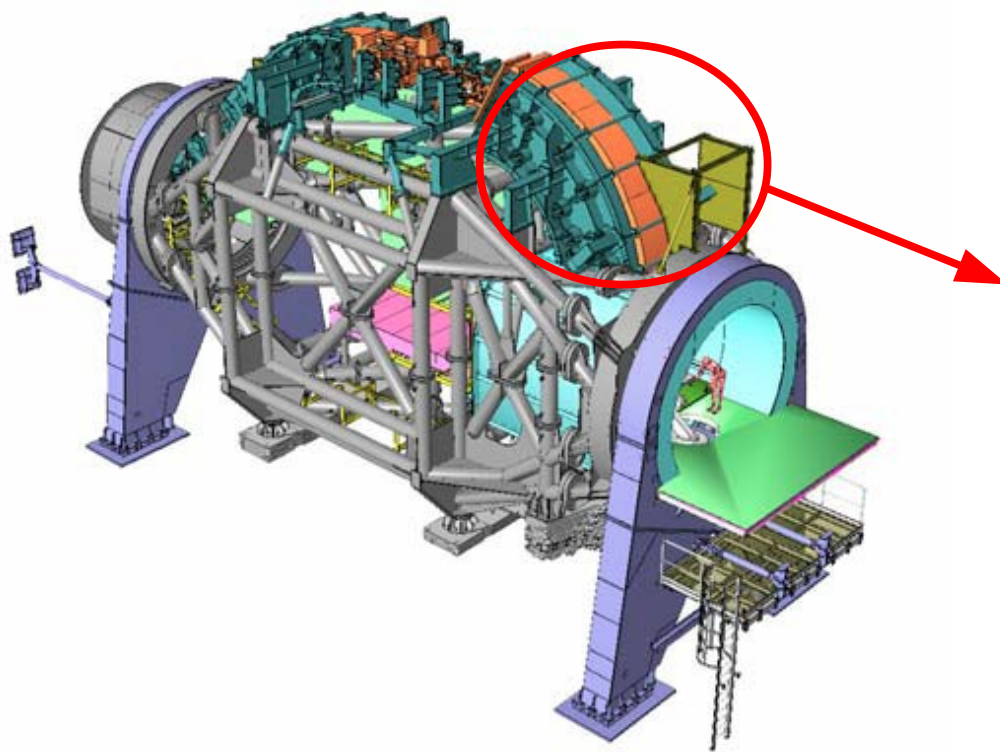


$\beta_L: 0.9\text{m}$, $\beta_H: 15\text{m}$, QFA=3.35, QD11=-3.05, QF11=3.31, QF21=2.95, QD21=-2.21, QD22=-1.19, QF22=2.02, QF31=2.39, QD31=-2.27, QFA1=3.17, QFD=-0.04

Outline of the Talk

- Multi-Objective Genetic Algorithms (MOGA)
- Applications at ALS
 - Low emittance lattice design and optimization for ALS upgrade
 - Curved superconducting combined-function magnet design
 - Spreader design and optimization for NGLS
- Electron beam diagnostics using Compton scattering technique

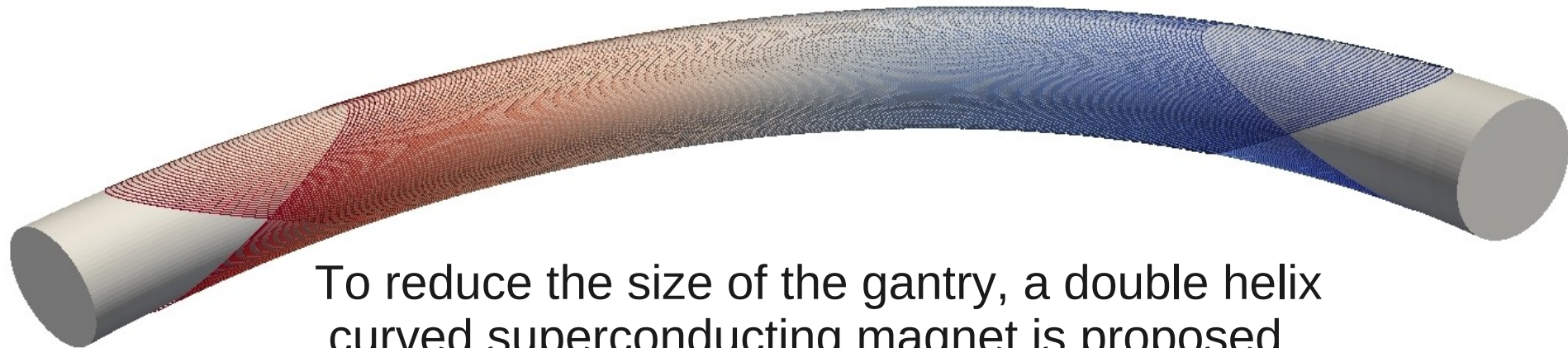
Ion Beam Therapy Gantry



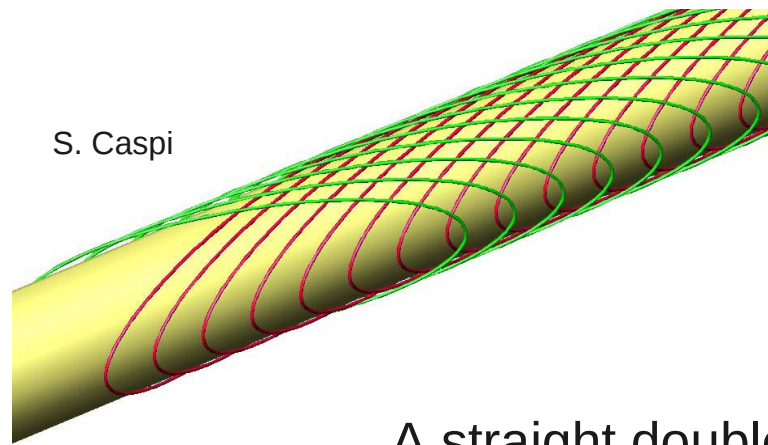
HIT 90 degree bend weigh 90 tons, 65% of total gantry weight

The final 90 degree bend drives the size and cost!!!

Curved Superconducting Magnet

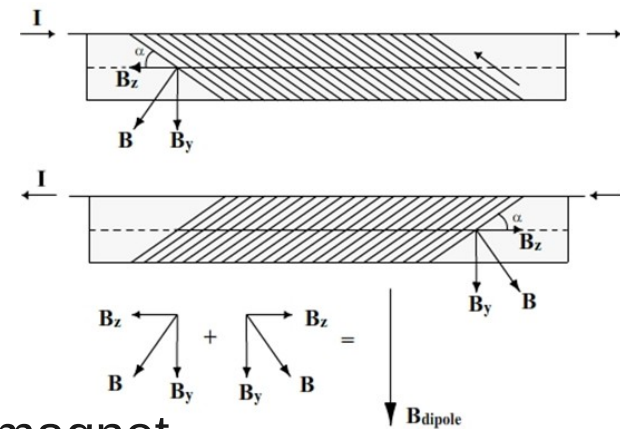


To reduce the size of the gantry, a double helix curved superconducting magnet is proposed.



A straight double helix magnet

- Two layer helical wire wound on a cylinder
- Solenoid magnet component are canceled
- Transverse field are doubled



Magnetic Fields Requirements

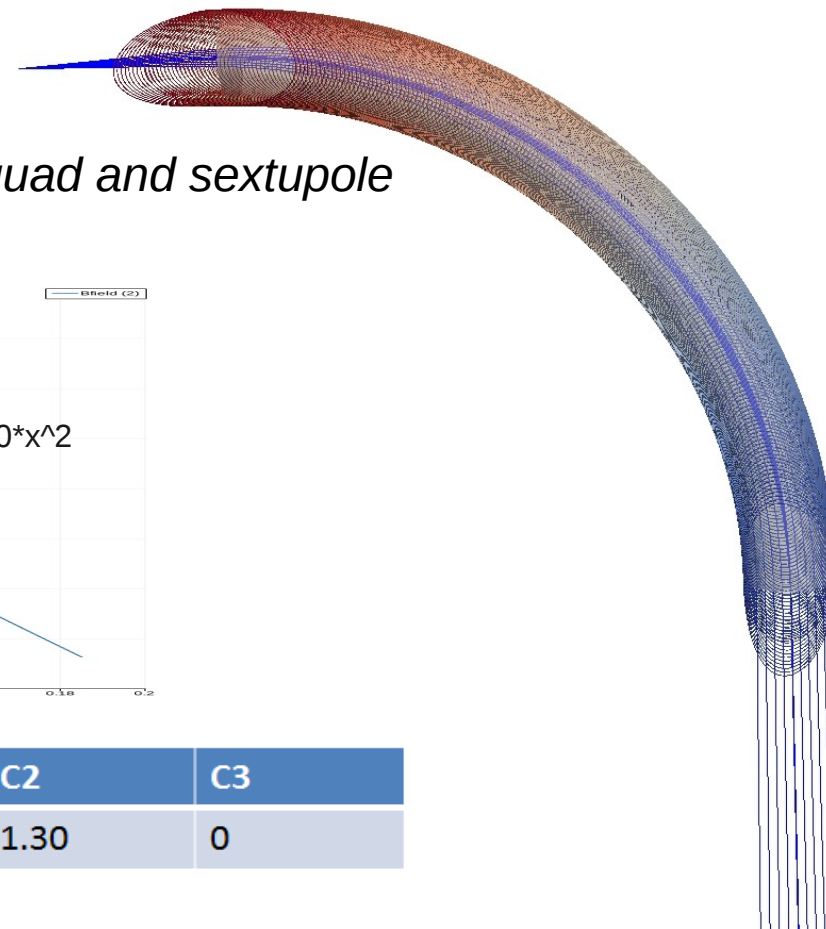
Scanning requirements:

1. point-to-parallel scanning
2. Minimize beam size distortion

The magnetic field with dipole, quad and sextupole components is needed.



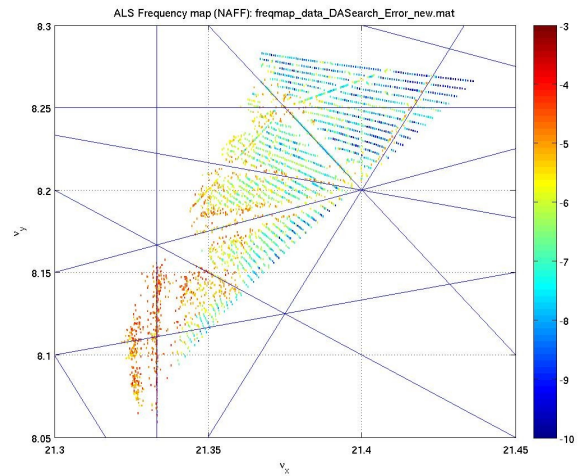
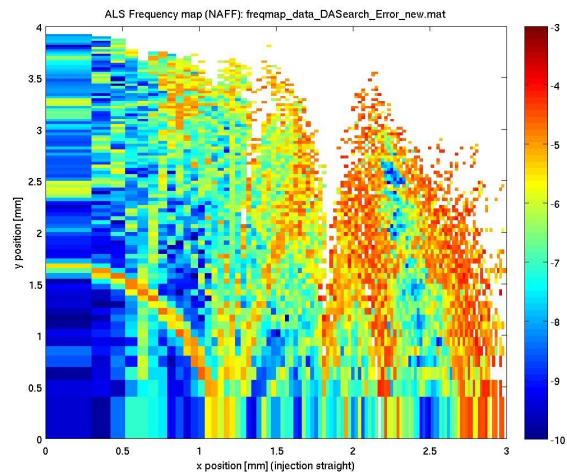
	C0	C1	C2	C3
"Ideal"	5.0000	-2.26	1.30	0



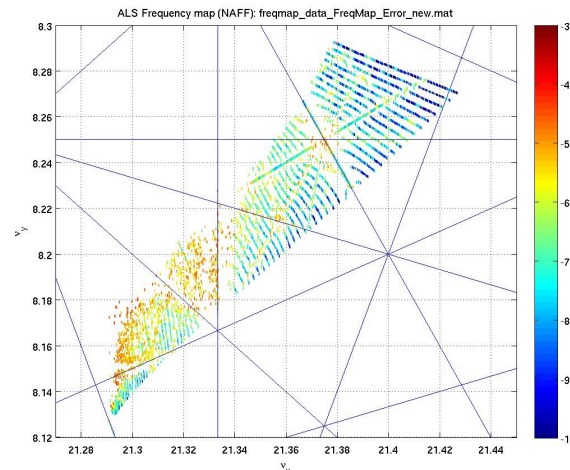
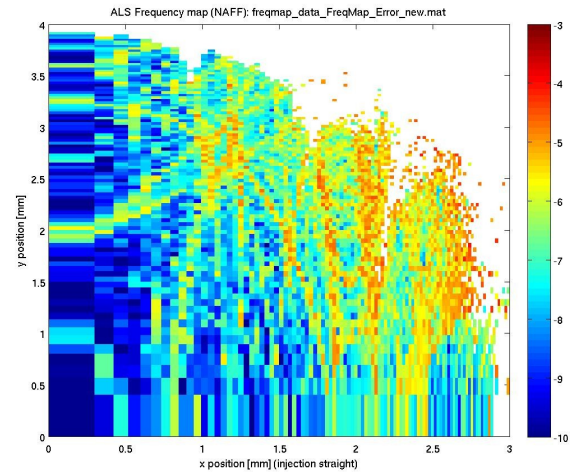
Challenges:

How to wind the wire on the torus to generate the required the multi-pole field components?

Frequency Map



Dyna. Ape. Area



Tot. Diff. Rate

The optimization using diffusion leads to an excellent nonlinear dynamic performance!

Parameterizing Winding on Torus

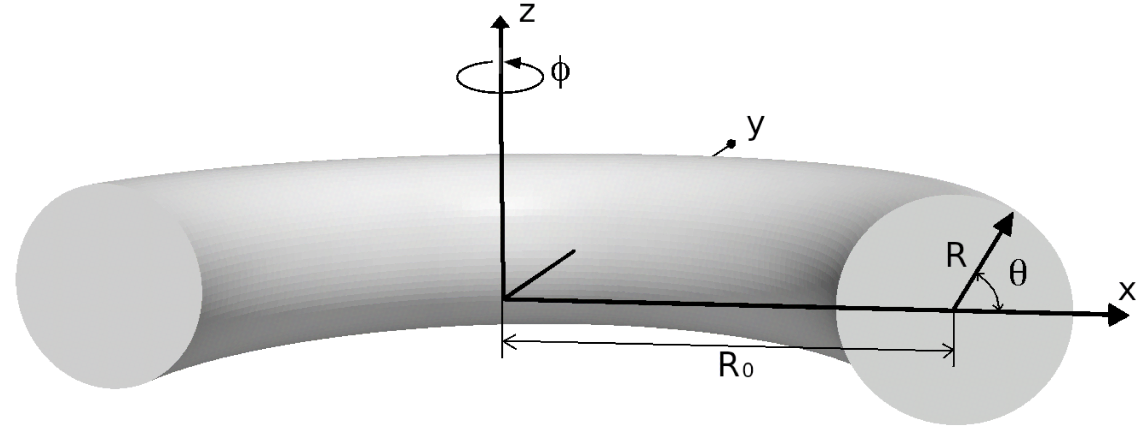
- A torus is generated by revolving a circle in 3D space about z-axis

- Coordinates on torus:

$$x = (R_0 + R \cos \theta) \cos \phi$$

$$y = (R_0 + R \cos \theta) \sin \phi$$

$$z = R \sin \theta$$



- Relation between ϕ and θ , $\phi = f(\theta)$, determine the winding path:

$$\phi = \theta/n + a_0 \sin \theta + a_1 \sin 2\theta + a_2 \sin 3\theta$$

Dipole

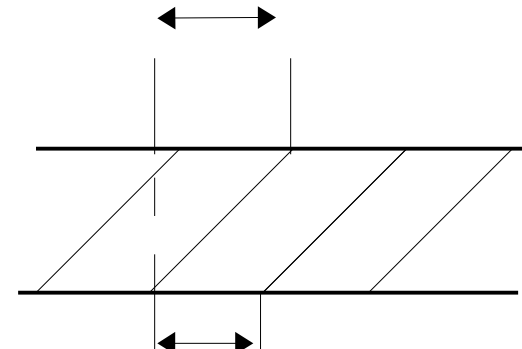
Quad

Sextupole

n : number of turns on a 2π torus, determining the pitch of each turn

a_0 : determine the angle of the wire with the horizontal plane, and large a_0 means small angle.

determined by a_0



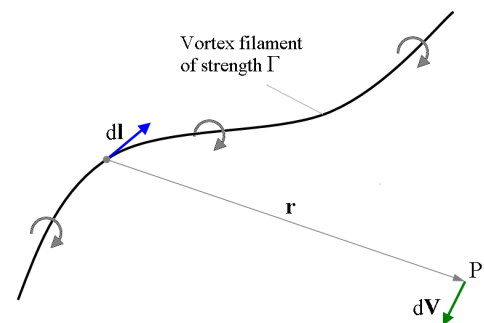
Pitch, determined by n

- Current path on torus

$$\begin{aligned}x &= (R_0 + R \cos \theta) \cos \phi & y &= (R_0 + R \cos \theta) \sin \phi & z &= R \sin \theta \\ \phi &= \theta/n + a_0 \sin \theta + a_1 \sin 2\theta + a_2 \sin 3\theta\end{aligned}$$

- Magnetic fields are calculated using Biot-savart law

$$\mathbf{B} = \int \frac{\mu_0}{4\pi} \frac{Idl \times \hat{r}}{|r|^2},$$

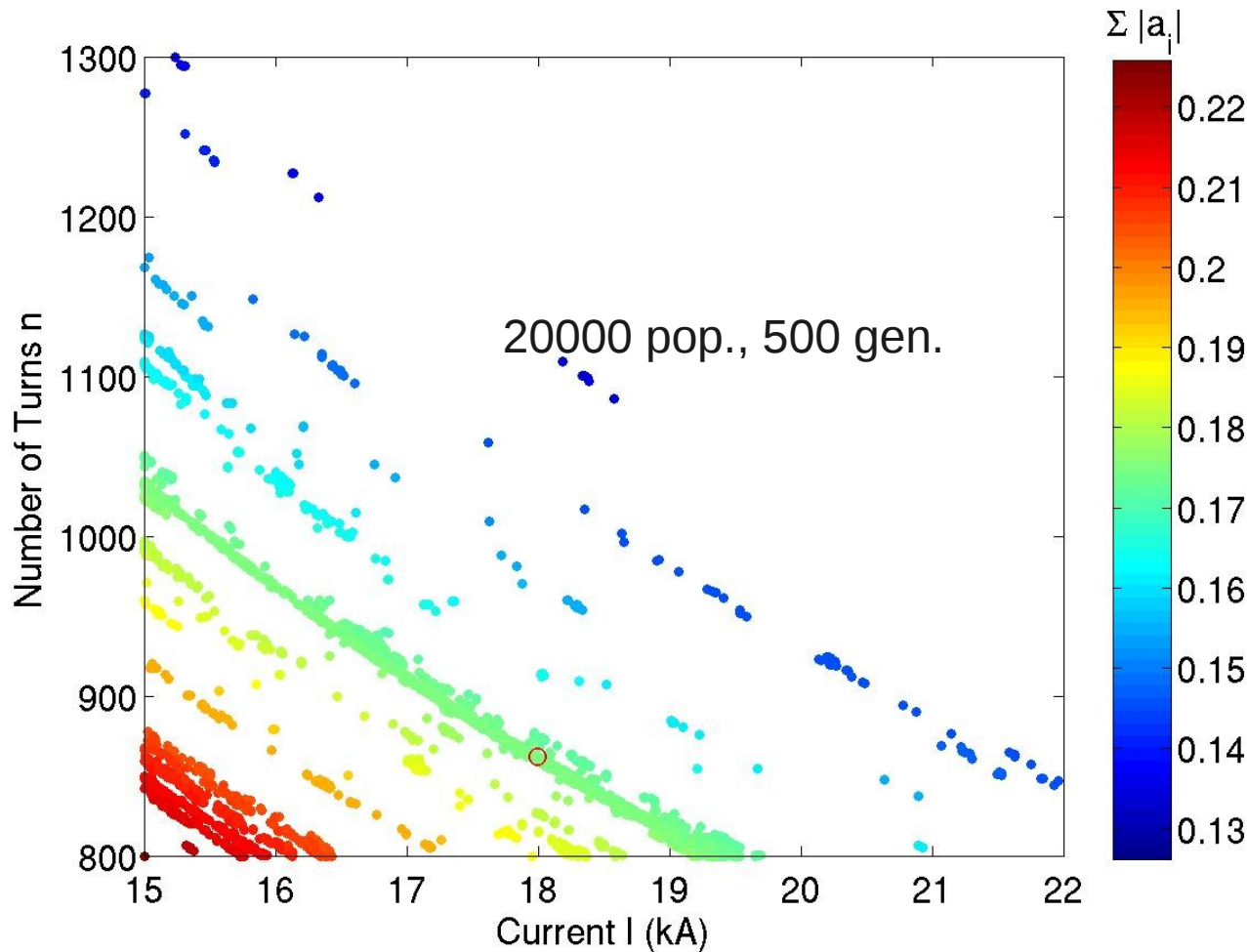


- Genetic solver:

- 5 parameters: I , n , a_0 , a_1, a_2
- 3 constraints: $\text{abs}(C_i' - C_i) < 0.05$, $i = 0, 1, 2$
- 3 objectives: less I , small n and $\text{abs}(a_0) + \text{abs}(a_1) + \text{abs}(a_2)$

	C0	C1	C2	C3
"Ideal"	5.0000	-2.26	1.30	0

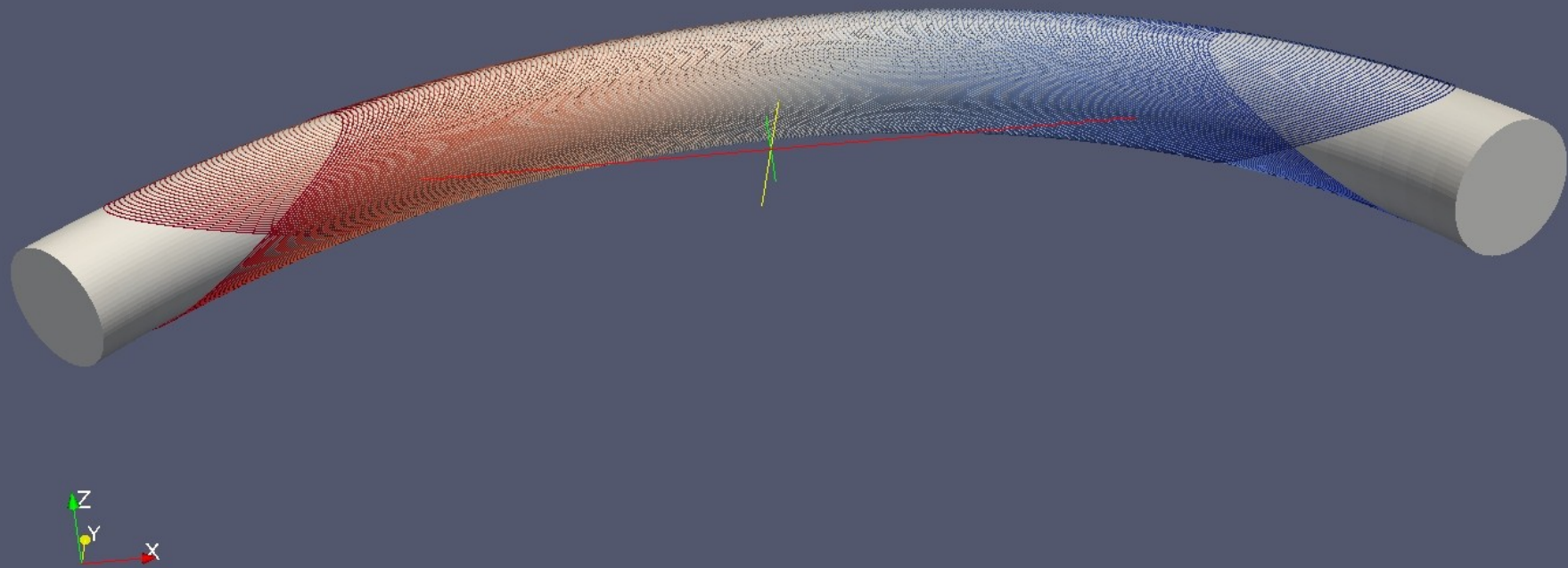
Optimal Solution Front



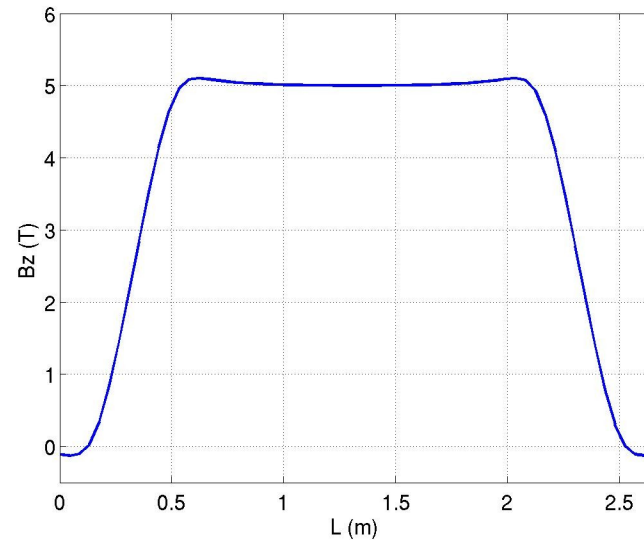
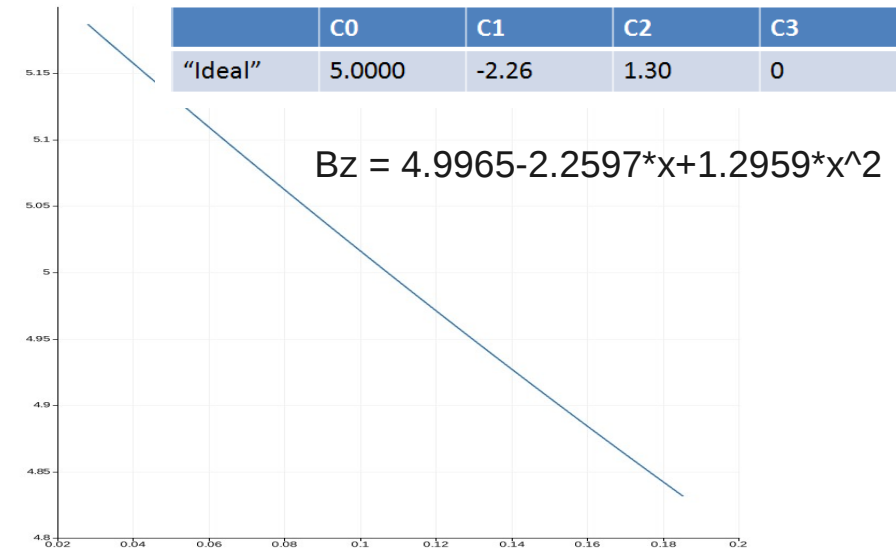
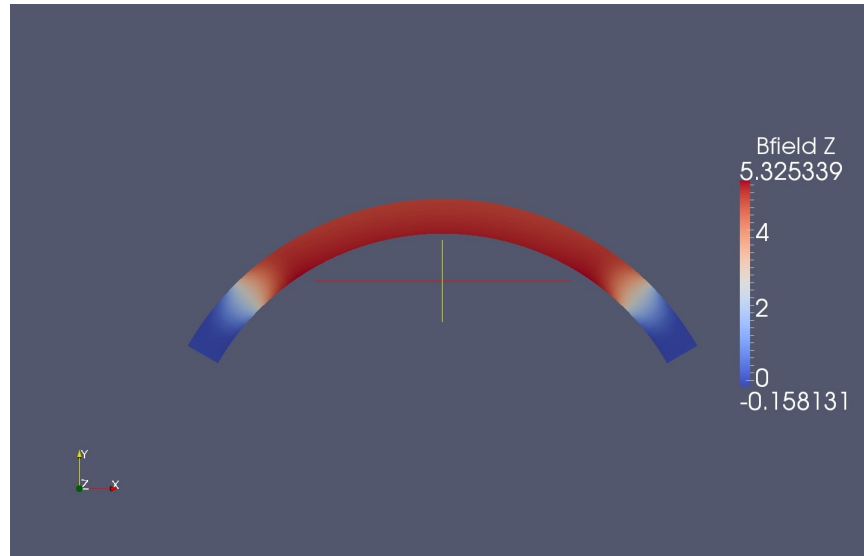
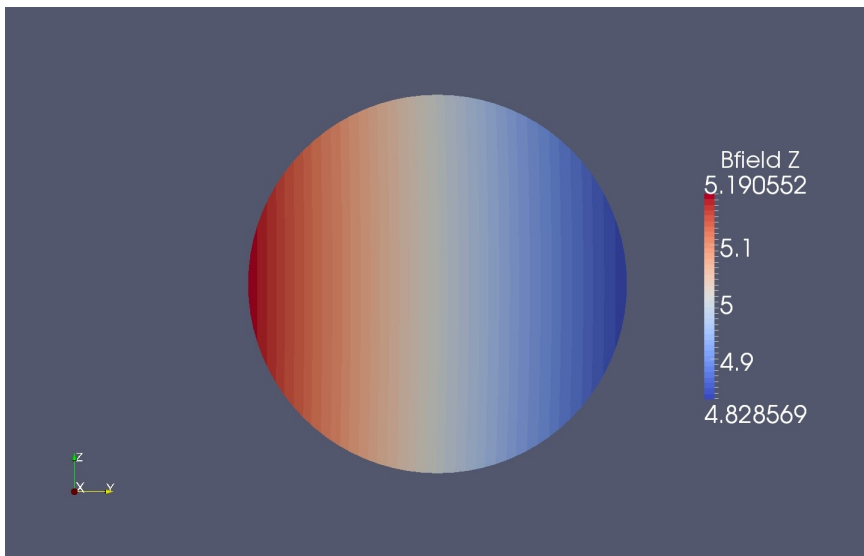
Trade-off between current I , winding turns n , and coefficient a_i :

- Less current, but more winding turns
- small a_i , but more current and winding turns

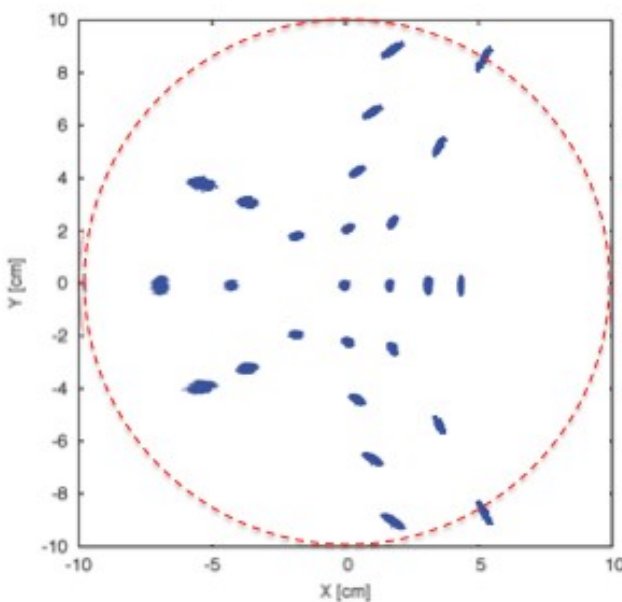
$I = 18 \text{ kA}$, $n = 216 \text{ turns}$, $a_0 = 0.168$, $a_1 = -5.74\text{e-}03$, $a_2 = 2.345\text{e-}04$
inner pitch: 8.5 mm, outer: 10 mm



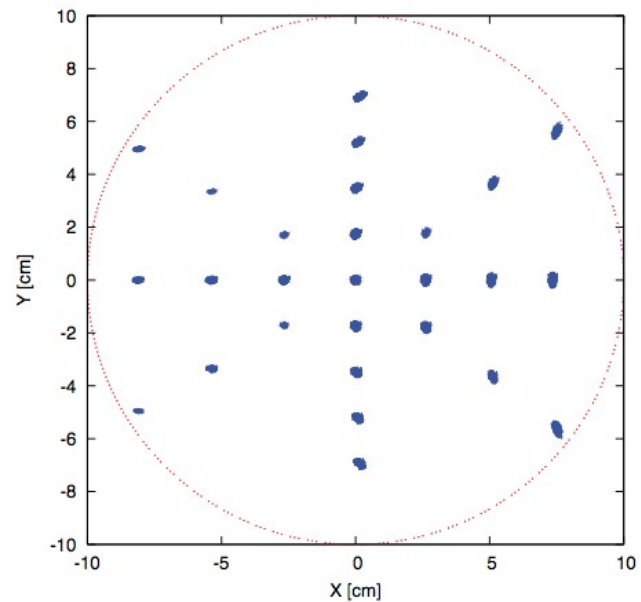
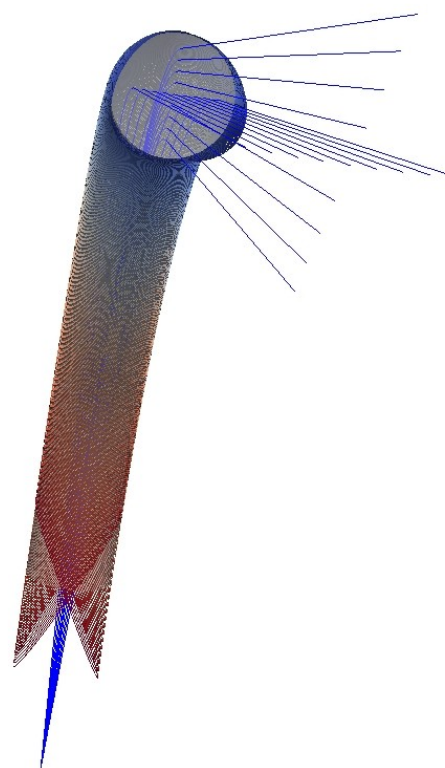
Magnetic fields



Scanned Beam Spots at Patient



Before optimization

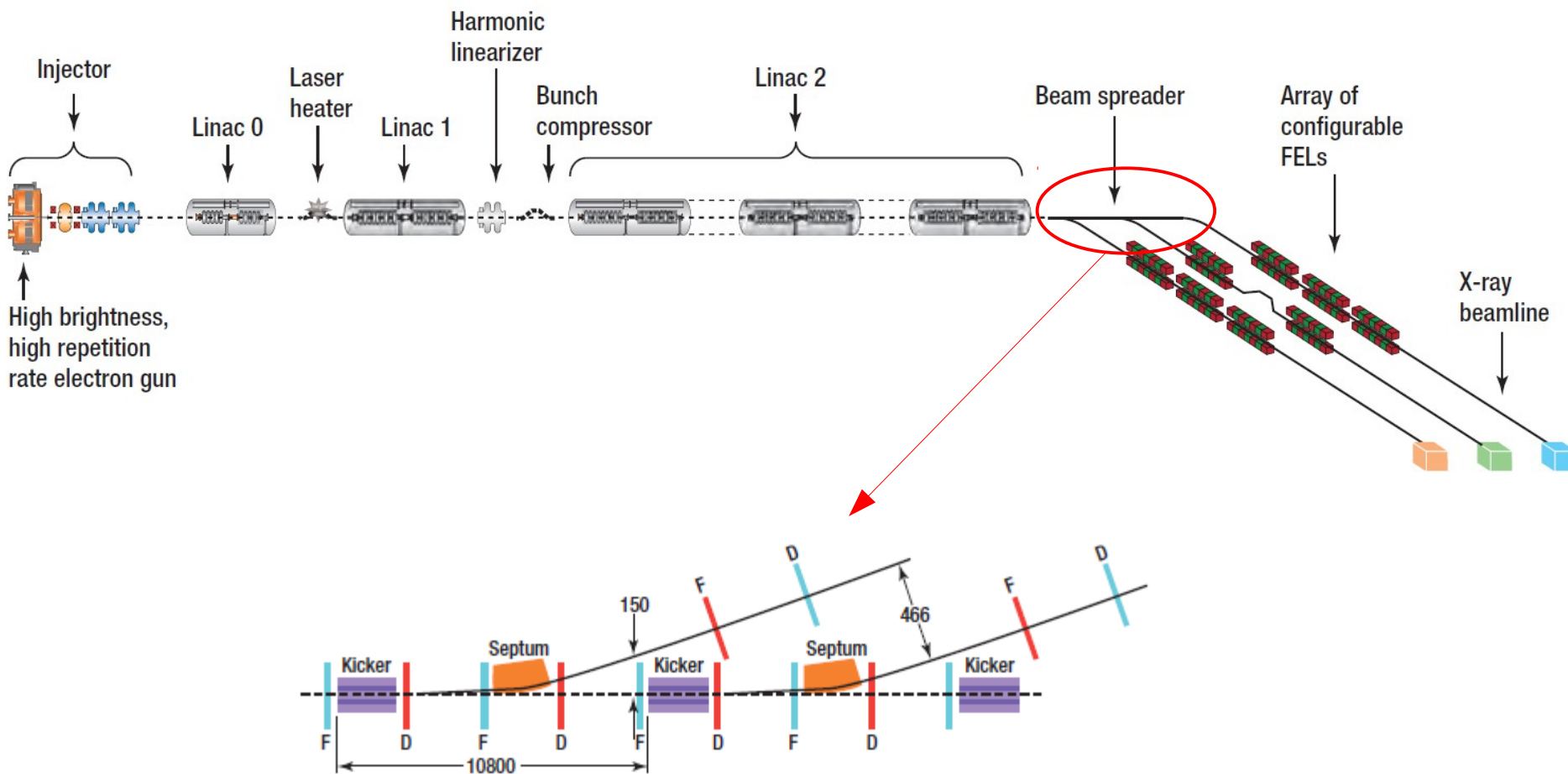


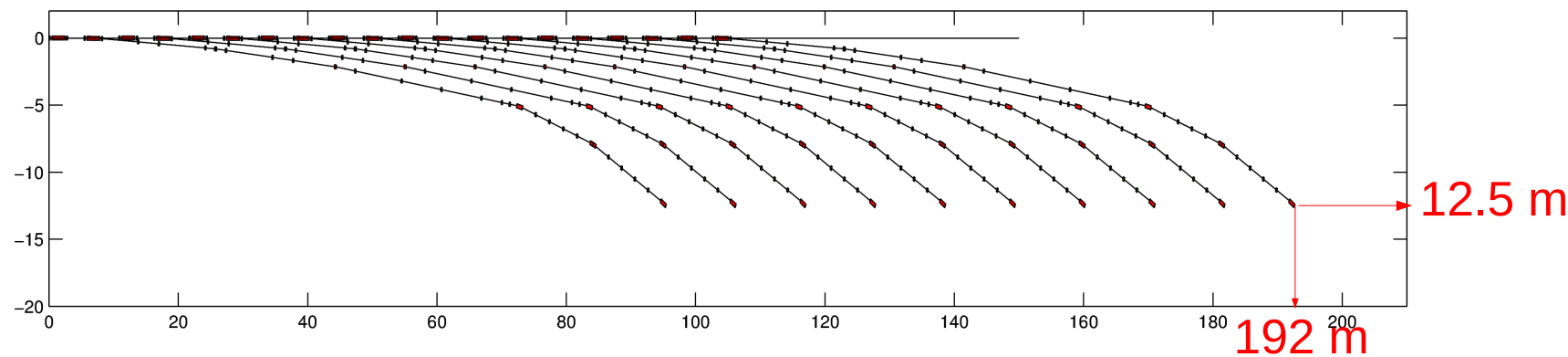
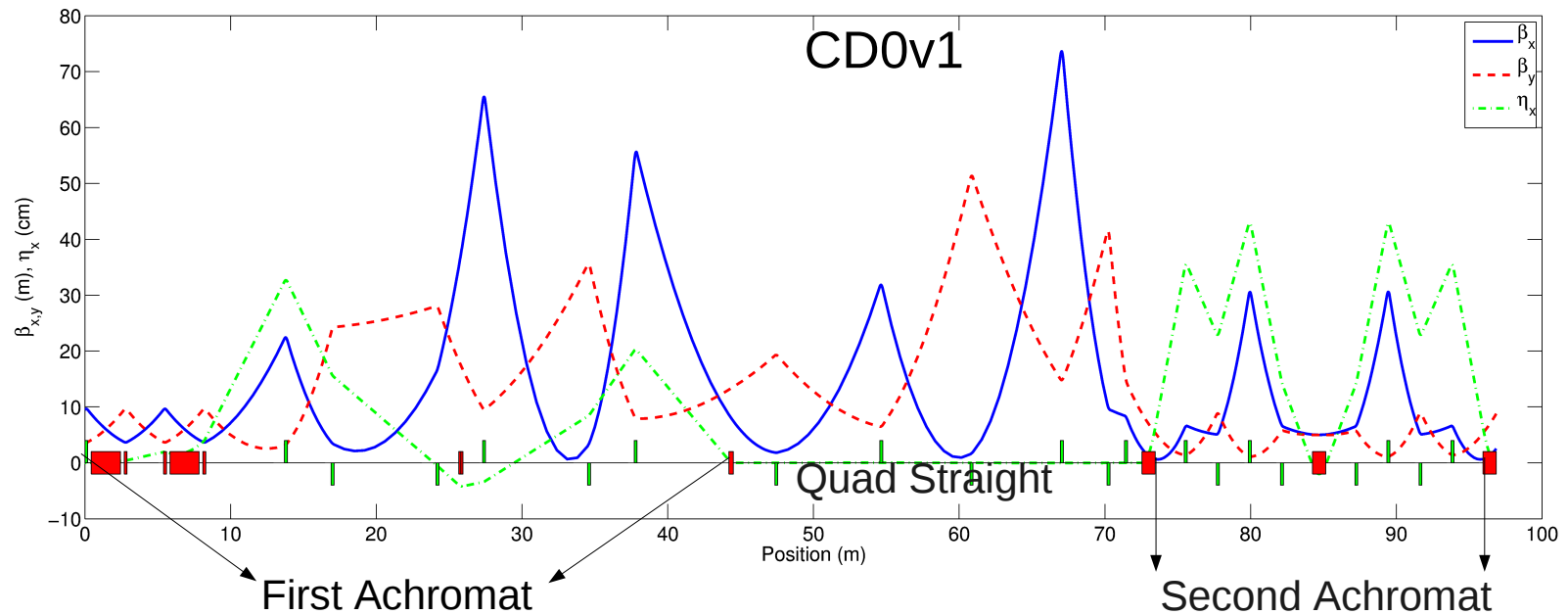
After optimization

Outline of the Talk

- Multi-Objective Genetic Algorithms (MOGA)
- Applications at ALS
 - Low emittance lattice design and optimization for ALS upgrade
 - Curved superconducting combined-function magnet design
 - Spreader design and optimization for NGLS
- Electron beam diagnostics using Compton scattering technique

NGLS Beam Spreader





Large footprint, doesn't fit the LBL site well, high real estate cost

Optimization of CD0 Design

- Optimization of the spreader is a multi-objective and multi-variable problem.
- Genetic Algorithm (GA) is well suitable to this task.
- The two achromats are optimized separately, and quad straight is used for the matching.

Objectives:

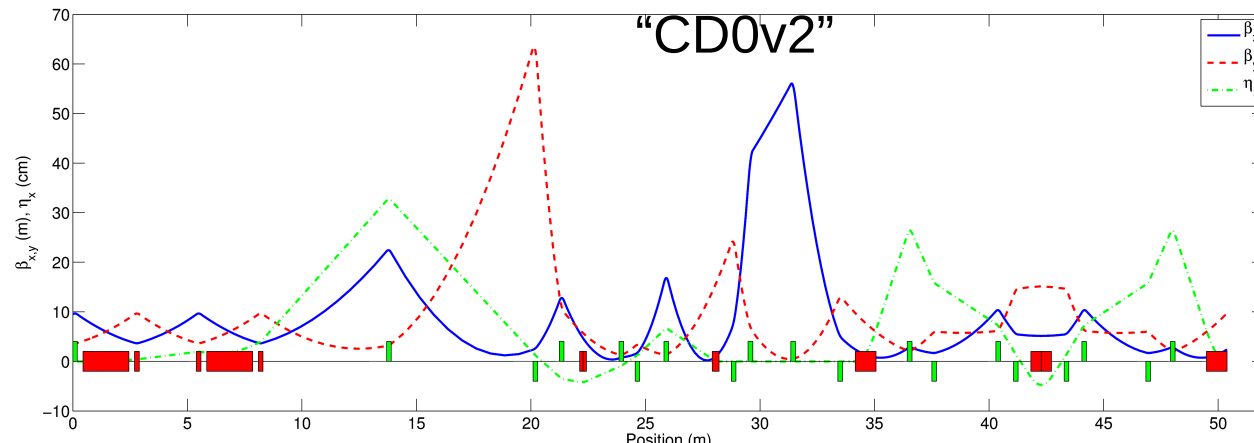
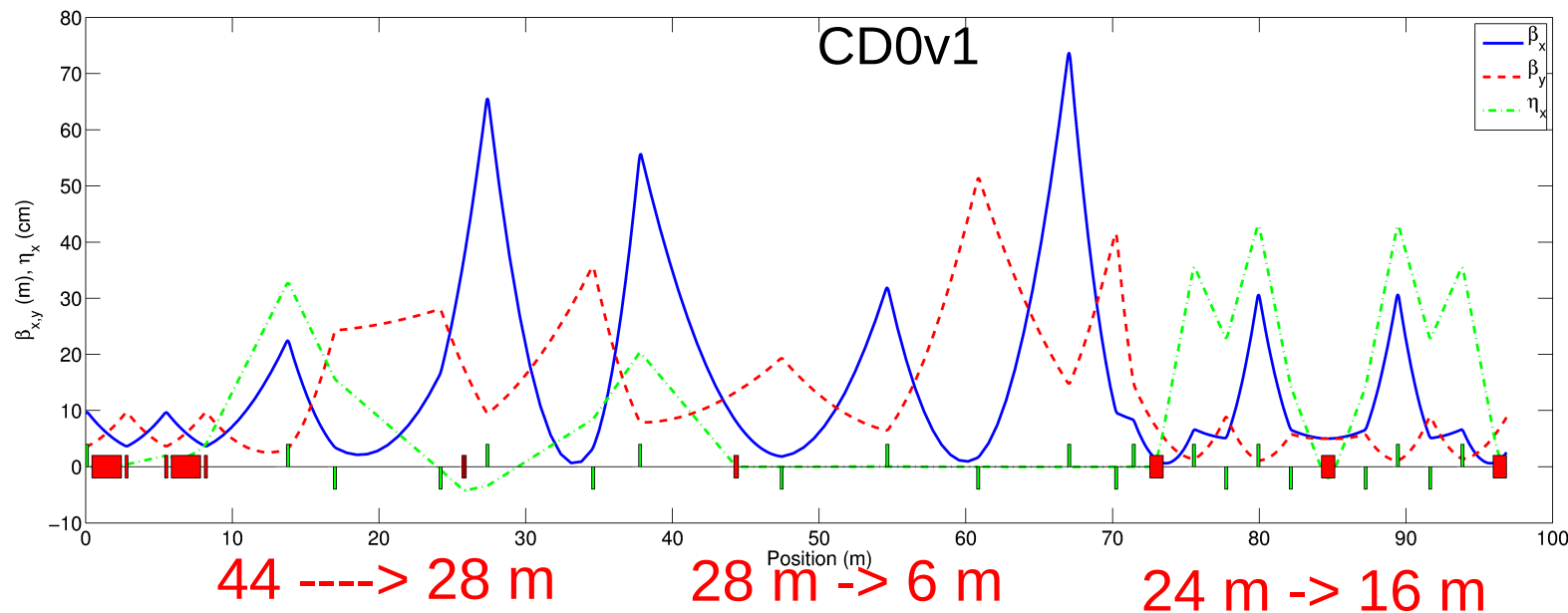
- Achromat: $R_{16}=R_{26}=R_{36}=R_{46}=0$
 - Isochronous: $R_{56}=0$
 - Dispersion free at the Quad straight: $\eta=\eta_{\text{ap}}=0$
 - Length of the arc
- } Evaluated using Differential Algebra (DA)

Constraints:

- Maximal beta function < 70 m and dispersion function < 50 cm

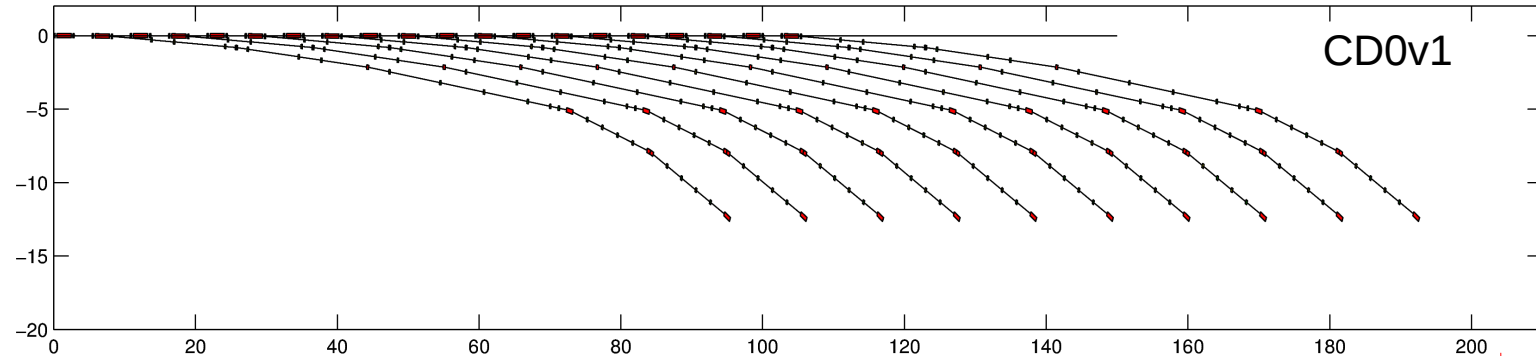
Variables:

- Quad strength and drift length.
- 14 variables for the first achromat and 9 variable for the second achromat

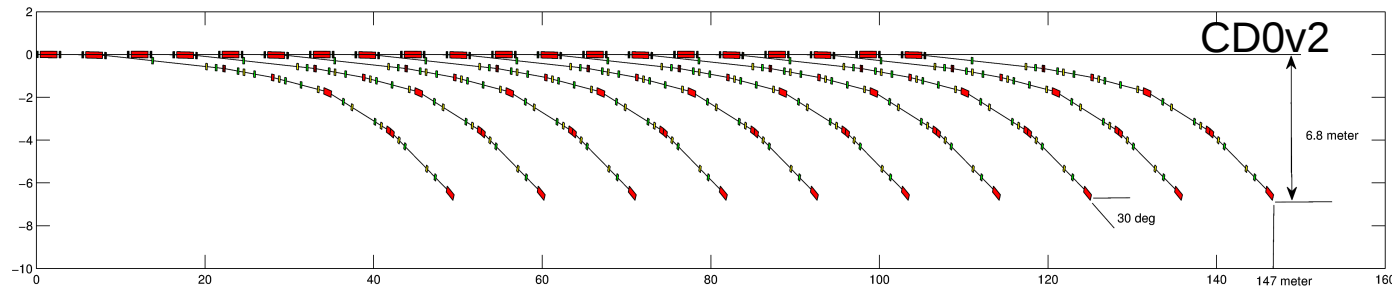


The new design (CD0v2) has the same performance to the original design in terms of CSR effects, magnet tolerance and high order chromatic effects.

Footprint Reduction



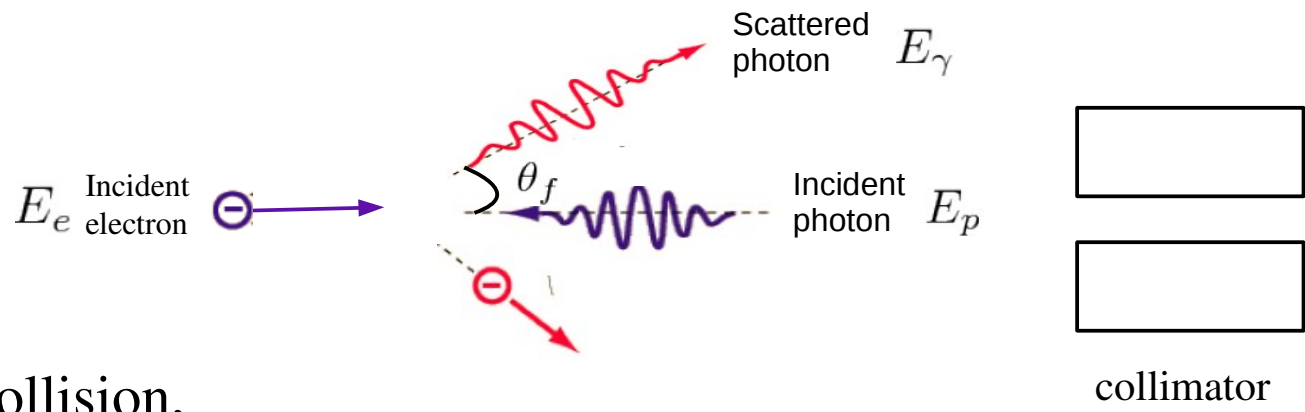
192 x12.5 m² -----> 147 x 6.8 m²



Outline of the Talk

- Multi-Objective Genetic Algorithms (MOGAs)
- Applications at ALS
 - Low emittance lattice design and optimization for ALS upgrades
 - Curved superconducting combined-function magnet design
 - Spreader design and optimization for NGLS
- Electron beam diagnostics using Compton scattering technique

Scattered Photon Energy



Head-on collision,

$$E_\gamma \approx \frac{4\gamma^2 E_p}{1 + \gamma^2 \theta_f^2 + 4\gamma^2 E_p/E_e}$$

Backscattering, $\theta_f = 0$

$$E_\gamma^{max} = \frac{4\gamma^2 E_p}{1 + 4\gamma^2 E_p/E_e}$$

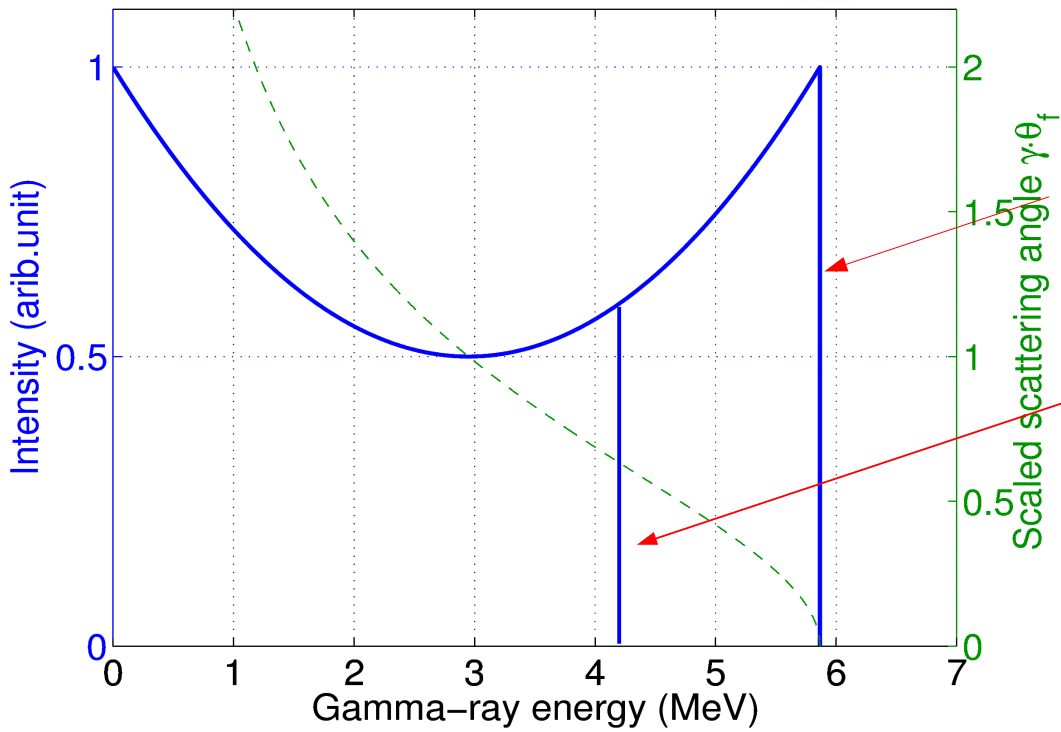
$$E_g^{max} \approx 4\gamma^2 E_p$$

Energy Spectrum of Scattered Photon Beam

For unpolarized/circularly polarized photons scattering with unpolarized electrons, the gamma-beam energy spectrum is given by

$$\frac{d\sigma}{dE_g} = \frac{8\pi r_e^2}{X(\beta E_e - E_p)} \left[\left(\frac{1}{X} - \frac{1}{Y} \right)^2 + \frac{1}{X} - \frac{1}{Y} + \frac{1}{4} \left(\frac{X}{Y} + \frac{Y}{X} \right) \right]$$

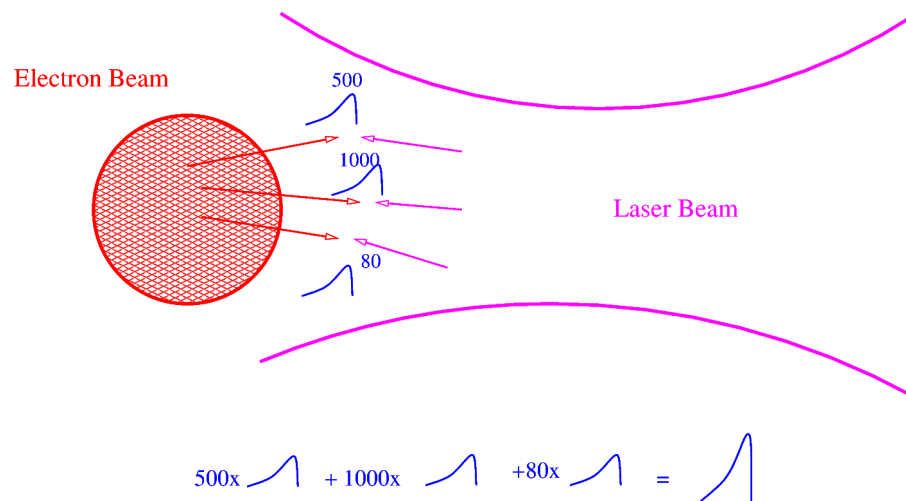
$$X = \frac{2\gamma E_p(1 + \beta)}{mc^2}, \quad Y = \frac{2\gamma E_g(1 - \beta \cos \theta_f)}{mc^2}$$



$$E_\gamma^{max} = \frac{4\gamma^2 E_p}{1 + 4\gamma^2 E_p/E_e}$$

$$E_\gamma \approx \frac{4\gamma^2 E_p}{1 + \gamma^2 \theta_f^2 + 4\gamma^2 E_p/E_e}$$

800 nm unpolarized laser photons scattering
500 MeV unpolarized electrons.



$$\frac{dN(E_g, x_d, y_d)}{d\Omega_d dE_g} \approx N_e N_p \int \frac{d\sigma}{d\Omega} \delta(\bar{E}_g - E_g) c(1 - \beta \cos \theta_i) f_e(x, y, z, x', y', p, t) f_p(x, y, z, k, t) dx' dy' dp dk dx dy dz dt$$

differential scattering
cross section

electron beam phase
space distribution

photon beam phase
space distribution

- Assuming Gaussian electron and laser beam:

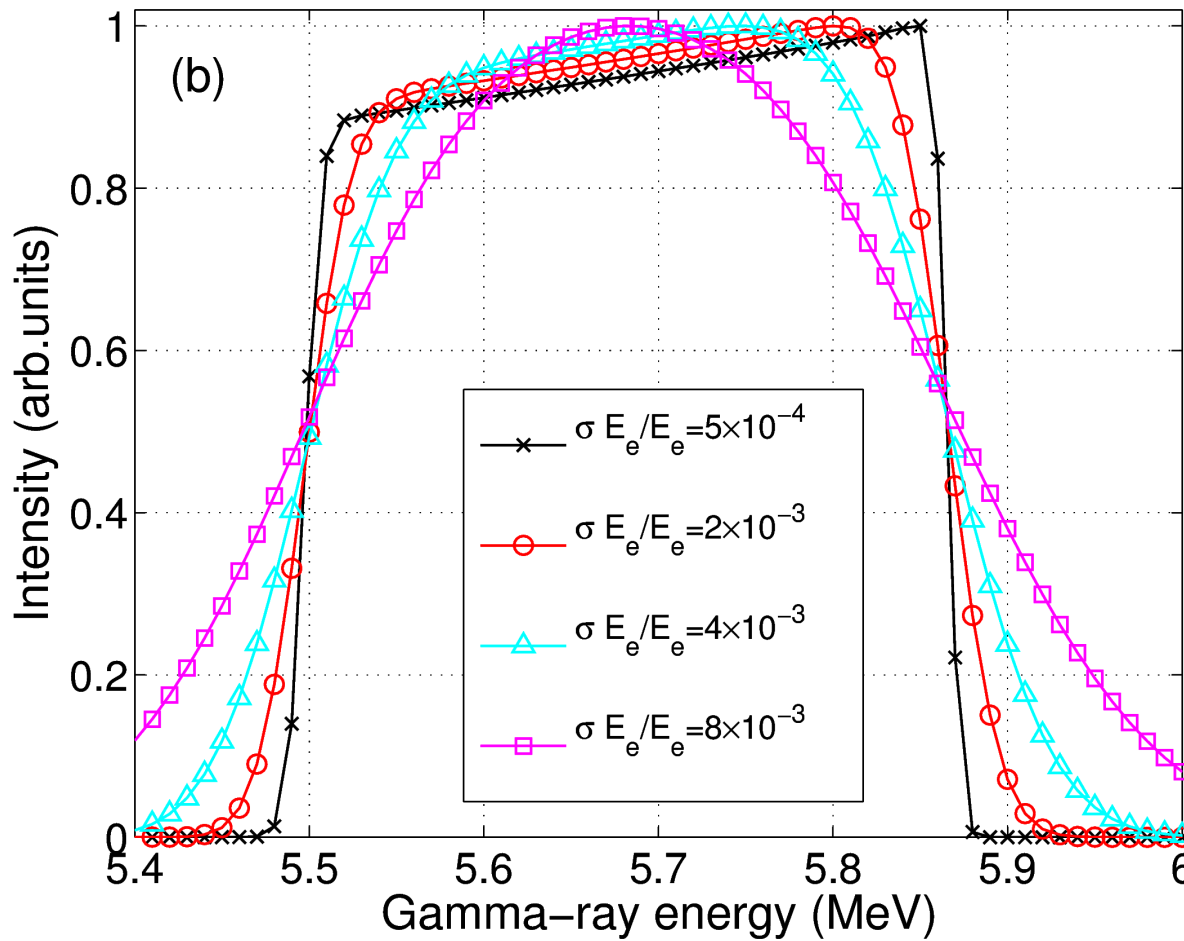
$$f_e(x, y, z, x', y', p, t) = \frac{1}{(2\pi)^3 \varepsilon_x \varepsilon_y \sigma_p \sigma_l} \exp \left[-\frac{\gamma_x x^2 + 2\alpha_x x x' + \beta_x x'^2}{2\varepsilon_x} \right. \\ \left. - \frac{\gamma_y y^2 + 2\alpha_y y y' + \beta_y y'^2}{2\varepsilon_y} - \frac{(p - p_0)^2}{2\sigma_p^2} - \frac{(z - ct)^2}{2\sigma_z^2} \right],$$

$$f_p(x_l, y_l, z_l, k, t) = \frac{1}{4\pi^2 \sigma_z \sigma_k \sigma_w} \exp \left[-\frac{x_l^2 + y_l^2}{2\sigma_w^2} - \frac{(z_l + ct)^2}{2\sigma_l^2} - \frac{(k - k_0)^2}{2\sigma_k^2} \right],$$

- Neglecting the vertical emittance of the electron beam and the energy spread of the laser energy beam, we can obtain:

$$\frac{dN(E_g, x_d, y_d)}{dE_g dx_d dy_d} \simeq \frac{r_e^2 L^2 N_e N_p}{2\pi^2 \hbar c \beta_0 \sqrt{\zeta_x} \sigma_\gamma \sigma_{\theta x}} \int_{-\theta_{x_{max}}}^{\theta_{x_{max}}} \frac{\gamma}{1 + 2\gamma E_p / mc^2} \left\{ \frac{1}{4} \left[\frac{4\gamma^2 E_p}{E_g(1 + \gamma^2 \theta_f^2)} + \frac{E_g(1 + \gamma^2 \theta_f^2)}{4\gamma^2 E_p} \right] \right. \\ \left. - \frac{\gamma^2 \theta_f^2}{(1 + \gamma^2 \theta_f^2)^2} \right\} \times \exp \left[-\frac{(\theta_x - x_d/L)^2}{2\sigma_{\theta_x}^2} - \frac{(\gamma - \gamma_0)^2}{2\sigma_\gamma^2} \right] d\theta_x, \quad (1)$$

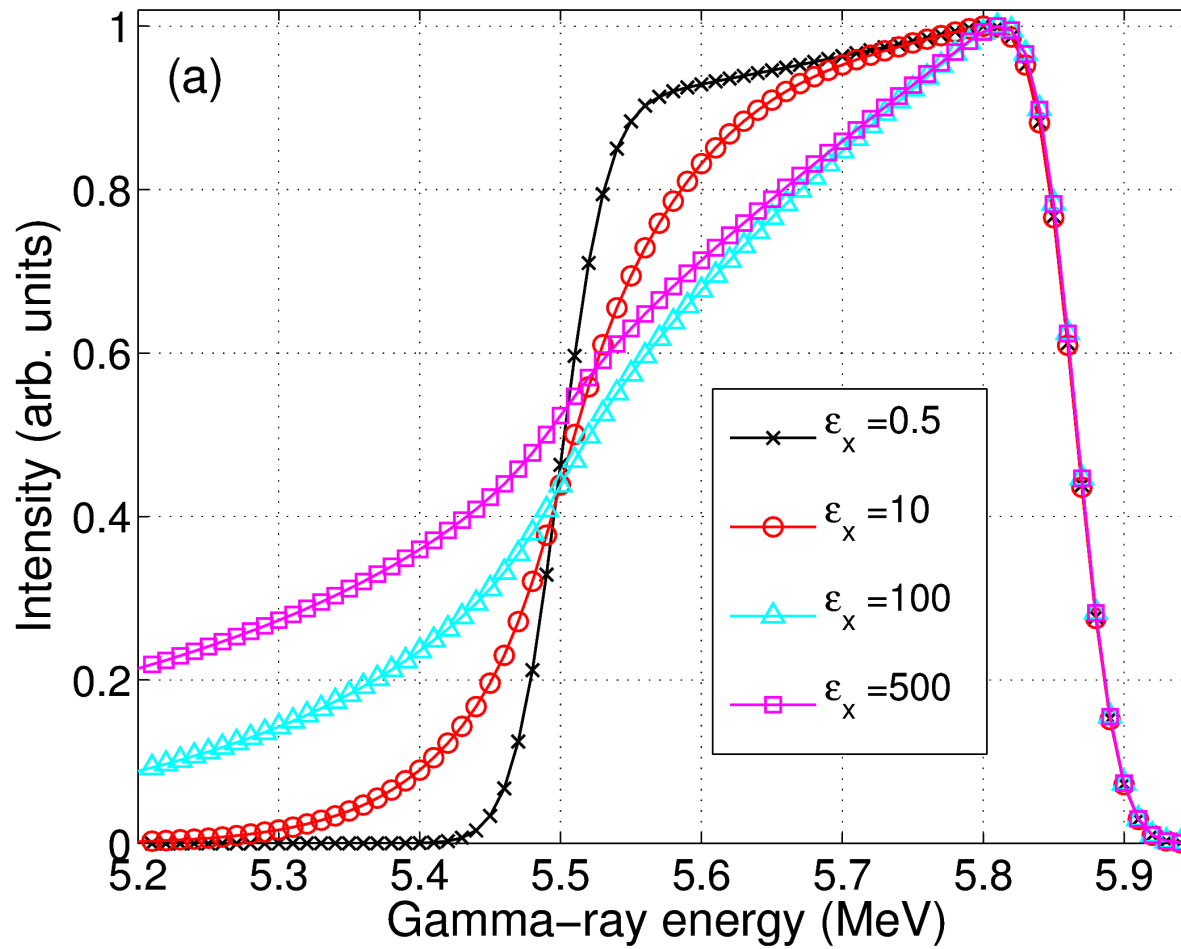
Effect of Electron Beam Energy Spread



500 MeV electron beam scattering with 800 nm laser beam, and the radius of the collimation aperture is 16mm

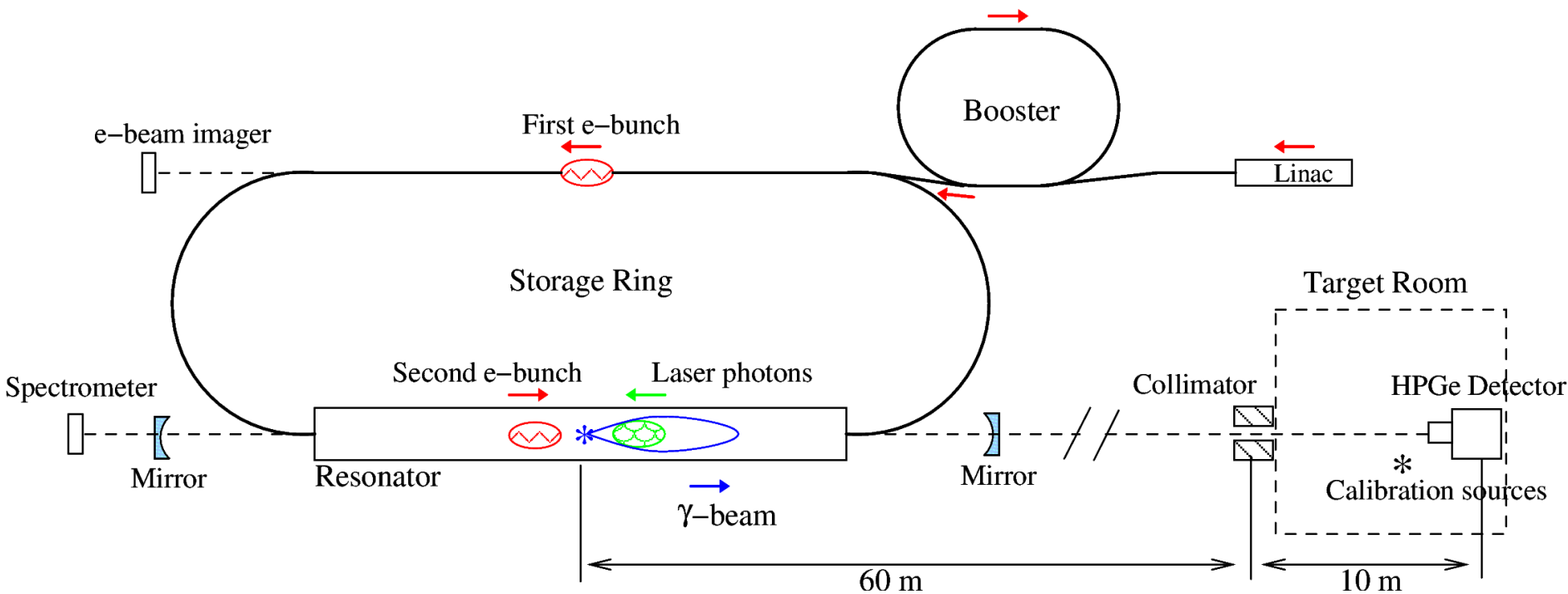
Both low and high energy edges are smeared due to the electron beam energy spread

Effect of Electron Beam Emittance

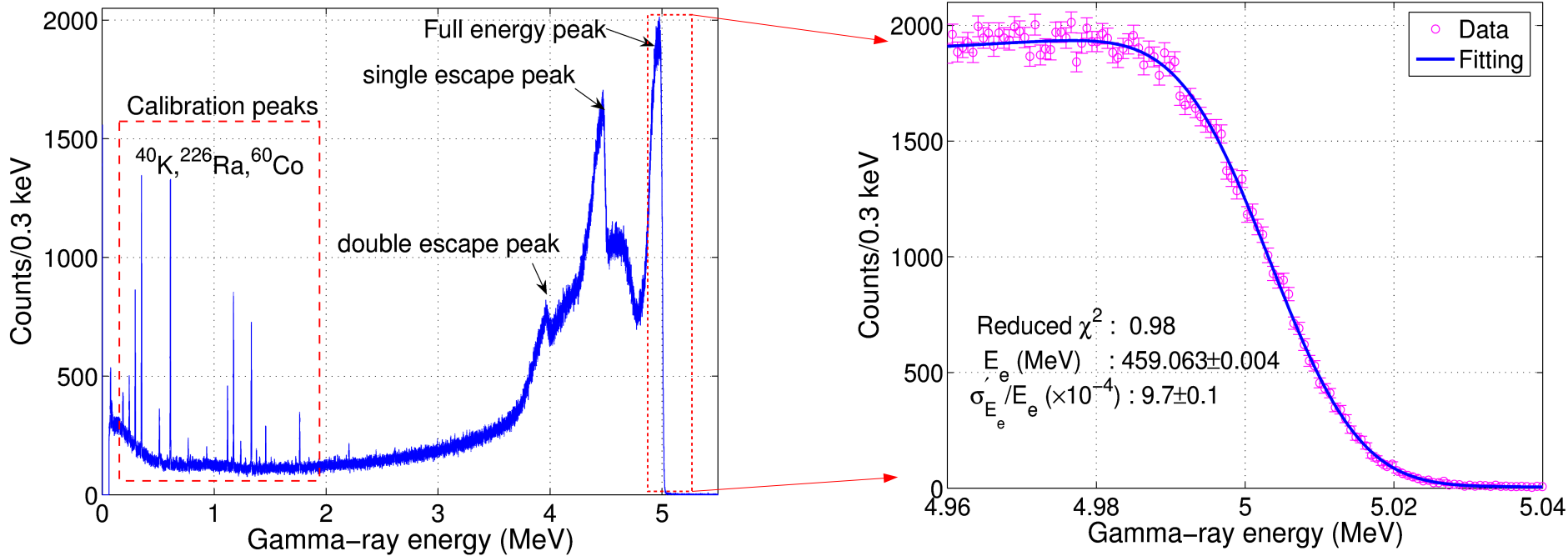


The electron beam emittance has no impact on the high energy edge of the spectrum if the collimation aperture is large enough.

HIGS: High Intensity Gamma-ray Source



Energy and Energy Spread Measurement



$$\frac{dN(E_g, x_d, y_d)}{dE_g dx_d dy_d} \simeq \frac{r_e^2 L^2 N_e N_p}{2\pi^2 \hbar c \beta_0 \sqrt{\zeta_x} \sigma_\gamma \sigma_{\theta_x}} \int_{-\theta_{x_{max}}}^{\theta_{x_{max}}} \frac{\gamma}{1 + 2\gamma E_p / mc^2} \left\{ \frac{1}{4} \left[\frac{4\gamma^2 E_p}{E_g(1 + \gamma^2 \theta_f^2)} + \frac{E_g(1 + \gamma^2 \theta_f^2)}{4\gamma^2 E_p} \right] - \frac{\gamma^2 \theta_f^2}{(1 + \gamma^2 \theta_f^2)^2} \right\} \times \exp \left[-\frac{(\theta_x - x_d/L)^2}{2\sigma_{\theta_x}^2} - \frac{(\gamma - \gamma_0)^2}{2\sigma_\gamma^2} \right] d\theta_x, \quad (1)$$

Apply Compton Scattering to NGLS?

- To measure electron beam energy at the end of the Linac, a long wavelength ($\lambda = 10.6$ micro, $E_p = 0.12\text{eV}$) CO₂ laser is needed.

$$E_g^{max} \approx 4\gamma^2 E_p$$

$$E_e = 2.4 \text{ GeV}, \gamma = 4696$$

$$E_g = 10.3 \text{ MeV}$$

→ Can be measured using HPGe detector

- The scattered photon flux is given by

$$\frac{dN_{tot}}{dt} = N_e N_p \mathcal{L}_{sc} \overline{\sigma_{tot}} f_0$$

$$\mathcal{L}_{sc} = \frac{1}{2\pi \sqrt{\frac{\lambda\beta_0}{4\pi} + \beta_x \varepsilon_x} \sqrt{\frac{\lambda\beta_0}{4\pi} + \beta_y \varepsilon_y}} = 2e5 \text{ m}^{-2} \quad \overline{\sigma_{tot}} = 6.65e-29 \text{ m}^2$$

$$\text{flux} = 4.2e9 \text{ Q(nC) P(kW)}, \text{ for } Q = 0.3 \text{ nC, } P = 1\text{kW}$$

$$\text{flux} = 1.3 e9 /sec$$

→ High enough

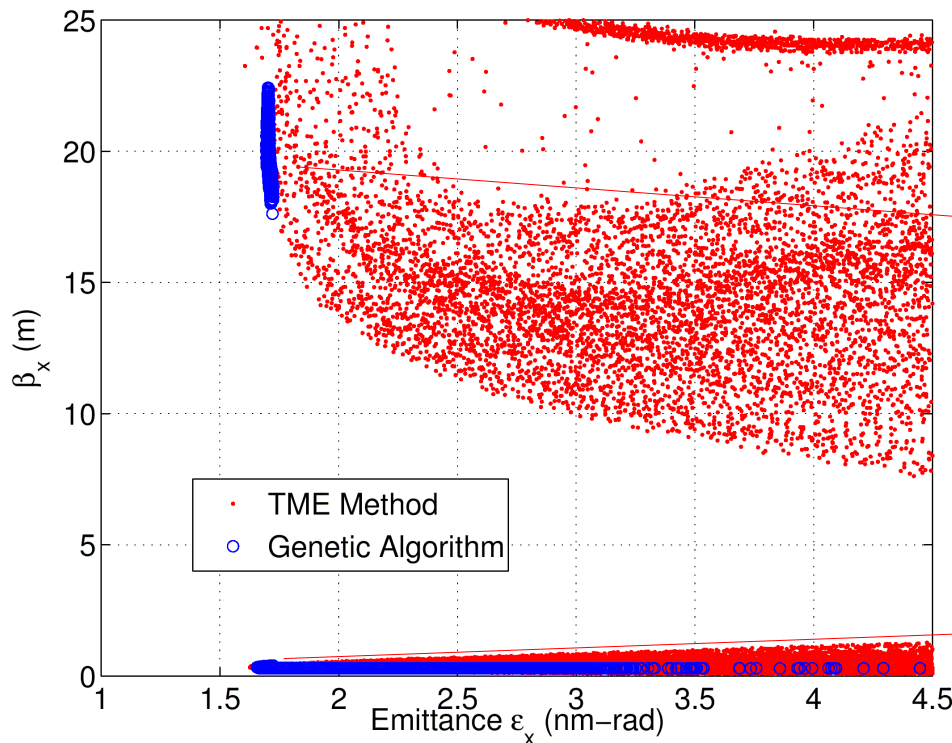
I have been involved in different projects at ALS including low emittance lattice design, dynamic aperture optimization and charged particle optics design.

I also experienced with diagnostics of electron beam using different technique such as Compton scattering and Toucheck Life time techniques.

Thanks!

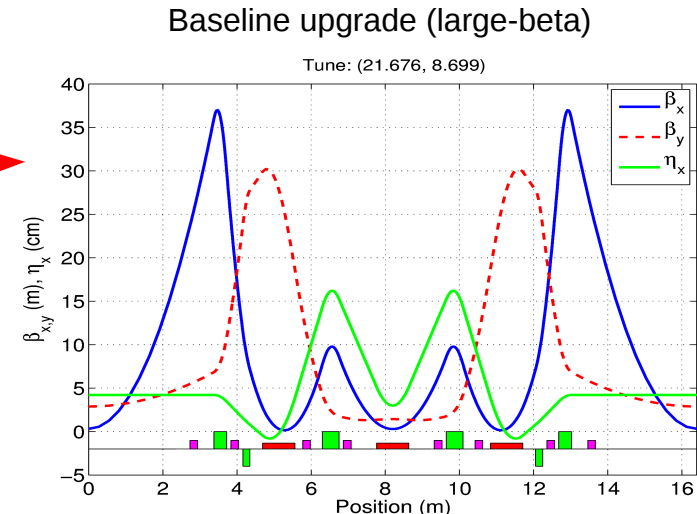
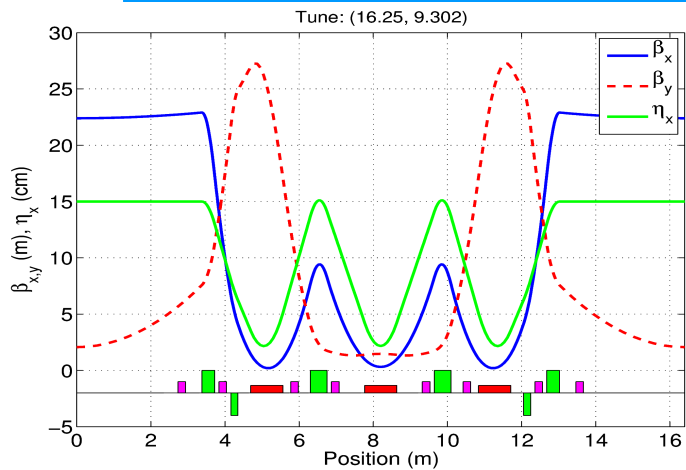
Backup slides

ALS lattice upgrades



- However, the ultimate upgrade lattice has small dynamic aperture, and is not compatible with traditional injection scheme due to a small beta at the straight. Optimization problems:

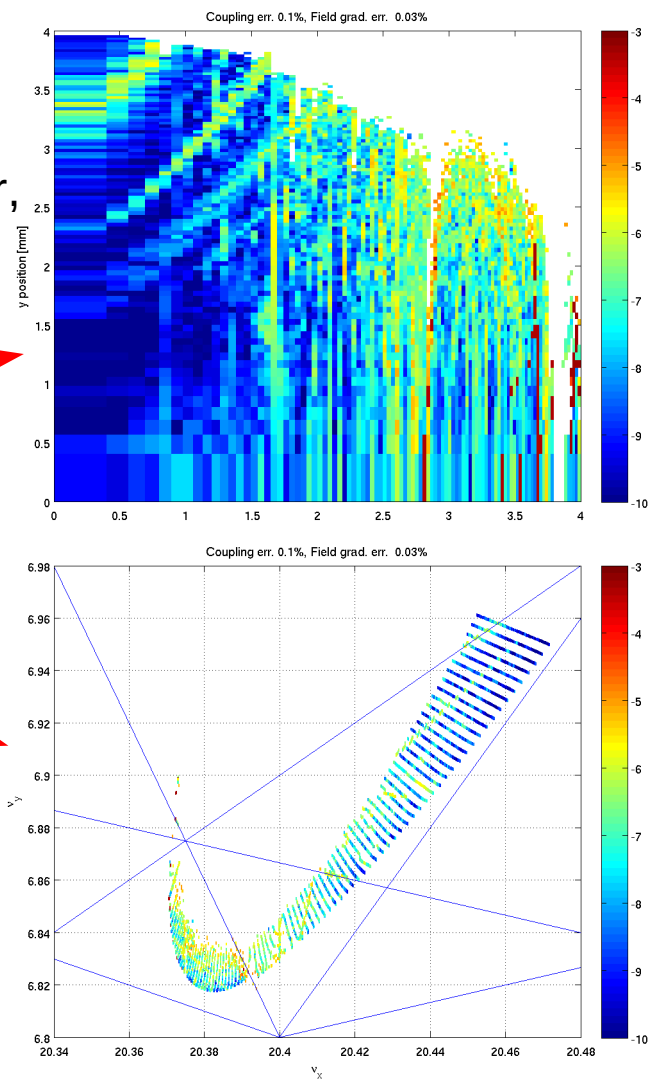
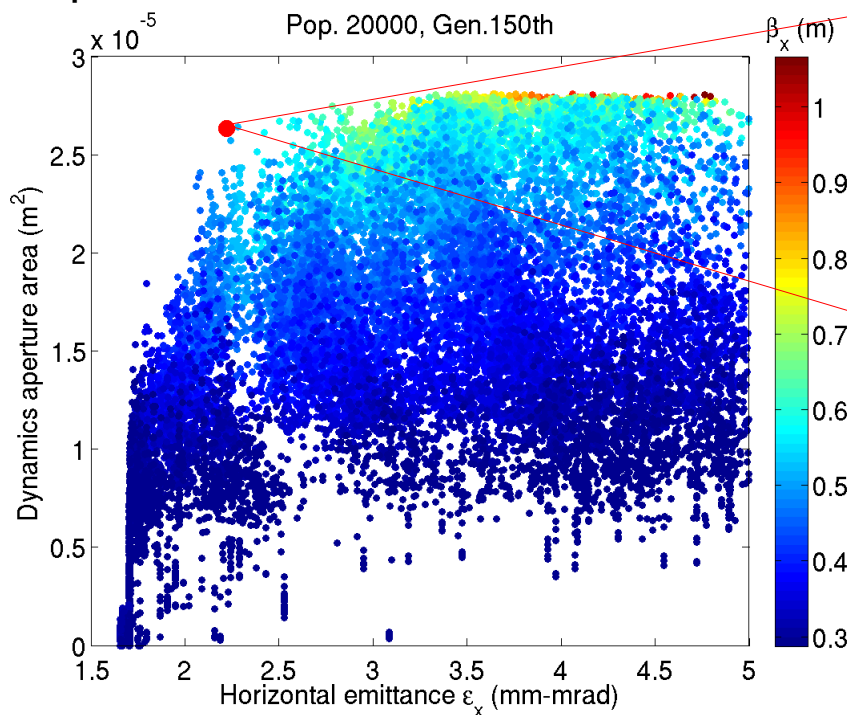
1. Dynamic aperture optimization
2. Alternating high and low beta lattice design



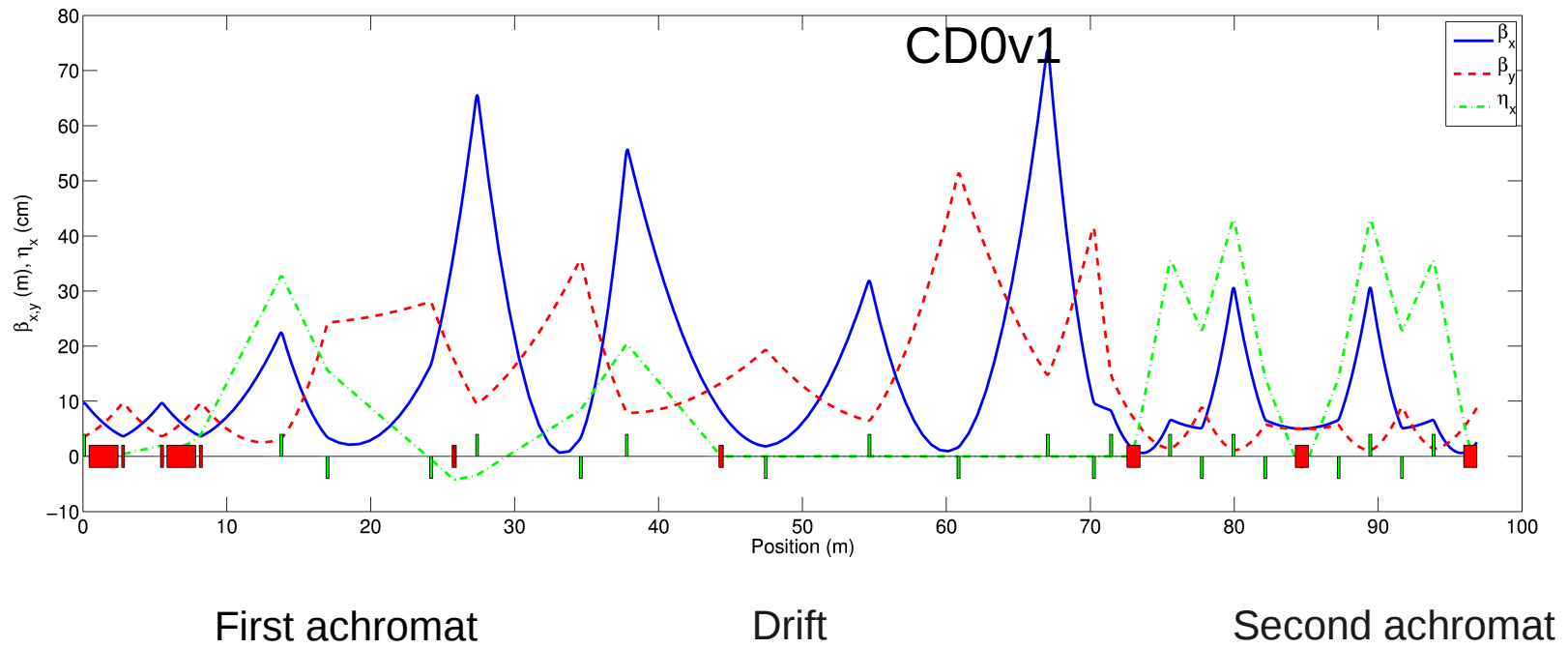
Simultaneous Linear and Nonlinear Optimization

Linear and nonlinear properties of the lattice are optimized simultaneously using GA.

- **7 parameters:** 3 Quads + 4 Sextupoles
- **7 constraints:** stability, positive partition number, maximum beta and dispersion functions
- **3 objectives:** emittance, betax and dynamics aperture



A trade-off between the dynamics and emittance is found.



- Keep the straight FODO lattice----10.8 meter per cell
- Keep the achromat structure ----- minimize the CSR effect
- Keep the first seven magnets' location and strength ---- the same space lim
- Keep all the bending magnet strength ----- 30 deg total bending angle
- **Vary the quad strength and drifts downstream of the first quad in the arc**
- **Optimize using Multi-objective Genetic Algorithm (MOGA)**

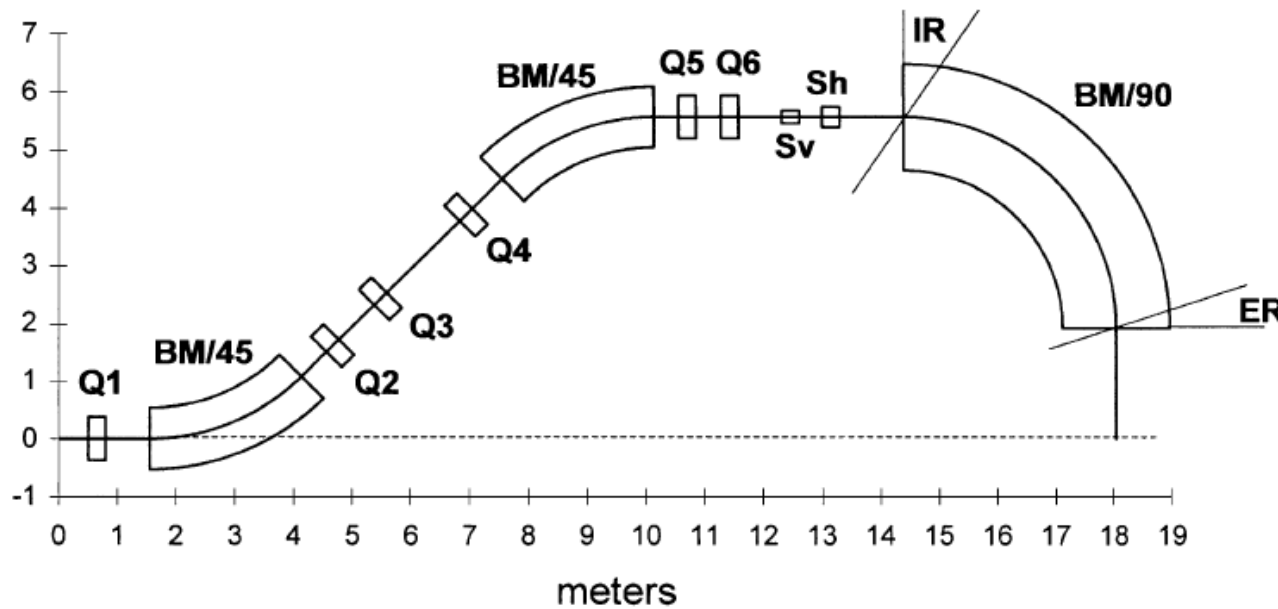
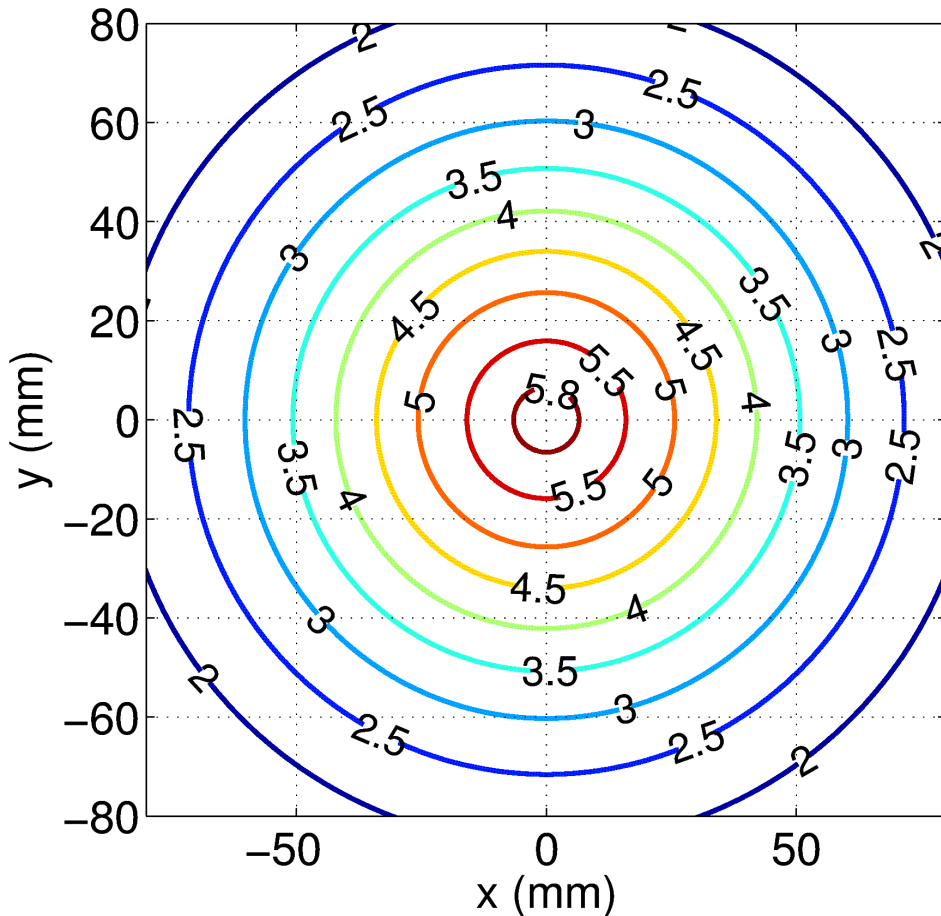


Fig. 3. Layout of the gantry with the minimum number of quadrupoles: Q1–Q6 = quadrupoles, BM/45 = 45° bending magnet, BM/90 = 90° bending magnet, Sh = horizontal scanner, Sv = vertical scanner, IR = input pole face rotation (30°), ER = exit pole face rotation (21°).



- 800 nm photon scattering with MeV electron, and the observation plane is 60 meters downstream from the collision point.
 - High energy gamma photon are peaked around the center.
 - Low energy gamma photon are distributed away from the center.

ALS Spectrum High Energy Edge

- Simple model [1]

$$\begin{aligned} f(E_\gamma, a_1, \dots, a_5) &= \int_0^\infty h(E_\gamma, E_\gamma^H) g(E_\gamma^H) dE_\gamma^H + a_5 \\ &\approx \frac{a_3}{\sqrt{2\pi}a_2} \int_{E_\gamma}^\infty [1 + a_4(E_\gamma - E_\gamma^H)] \times \exp\left(-\frac{(E_\gamma^H - a_1)^2}{2a_2^2}\right) dE_\gamma^H + a_5 \\ &= a_3 \left\{ \frac{1}{2} [1 + a_4(E_\gamma - a_1)] \times \operatorname{erfc}\left(\frac{E_\gamma - a_1}{\sqrt{2}a_2}\right) - \frac{a_2 a_4}{\sqrt{2\pi}} \times \exp\left(-\frac{(E_\gamma - a_1)^2}{2a_2^2}\right) \right\} + a_5 \end{aligned}$$

[1] R. Klein, T. Mayer, P. Kuske, R. Thornagel, and G. Ulm. Nucl. Instr. and Meth., A384:293–298, 1997.

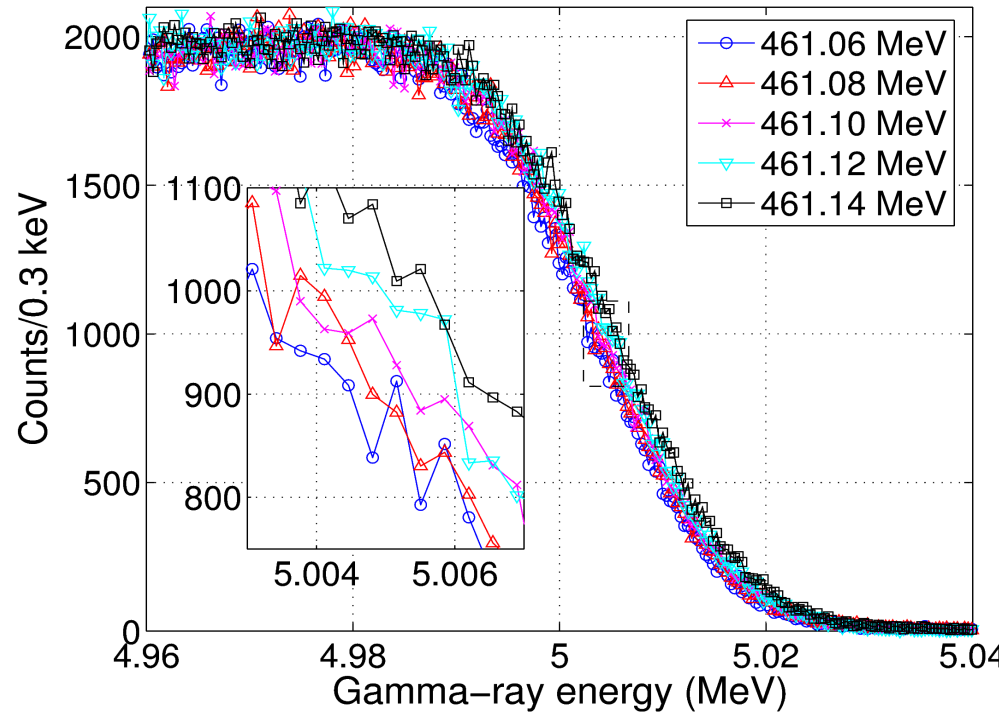
Gamma-beam collimation and electron beam emittance effects are neglected.

- Comprehensive model

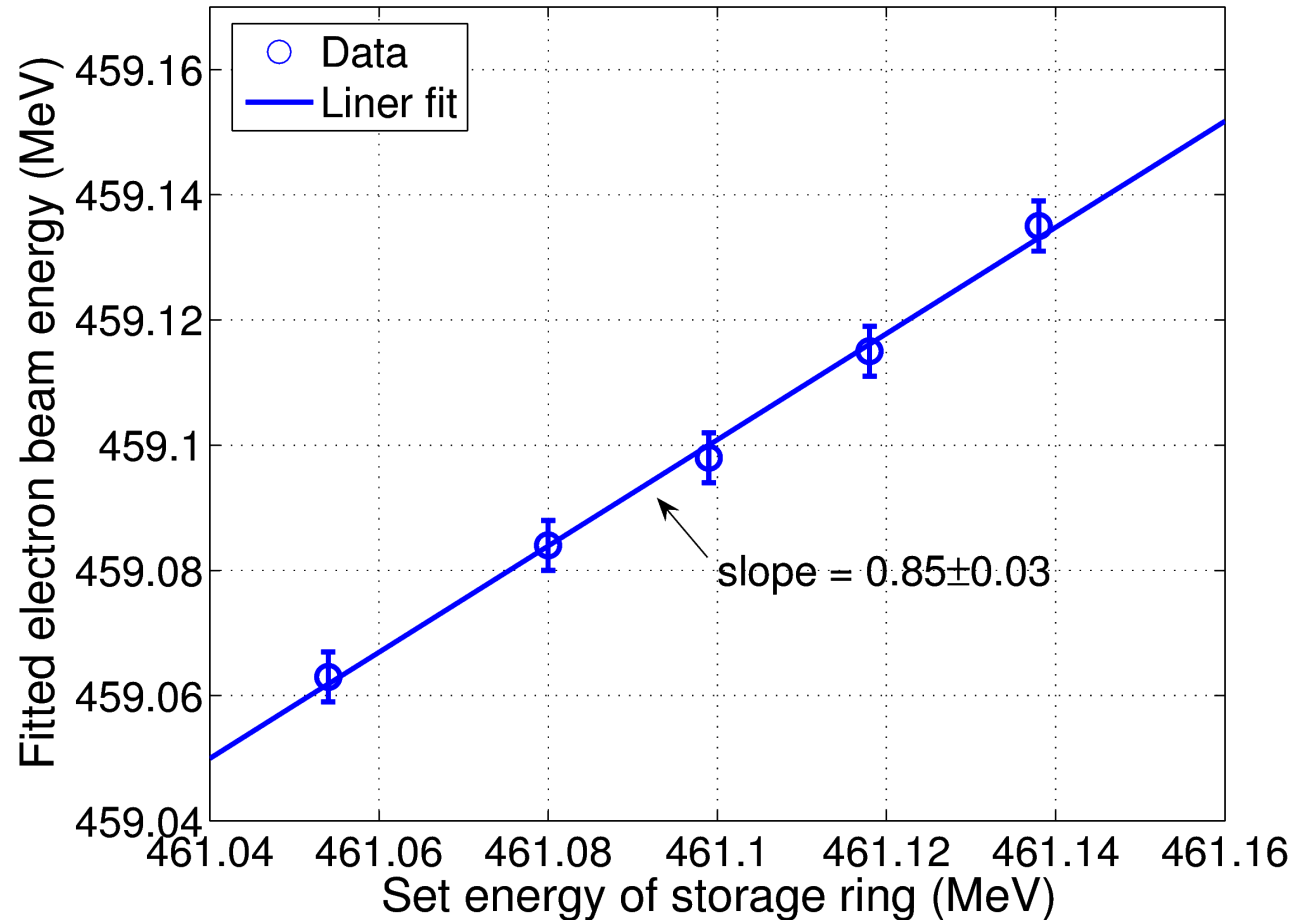
$$\begin{aligned} \frac{dN_\gamma}{dE_\gamma} \approx & \frac{r_e^2 L^2 N_e N_p}{2\pi^2 \hbar c \beta_0 \sqrt{\zeta_x} \sigma_\gamma \sigma_{\theta x}} \int_{-y_o}^{y_o} \int_{-x_o}^{x_o} \int_{-\theta_{x max}}^{\theta_{x max}} \left(\frac{\bar{\gamma}}{1 + 2\bar{\gamma}a} \right) \times \left\{ \frac{1}{4} \left[\frac{4\bar{\gamma}^2 E_p}{E_\gamma(1 + \bar{\gamma}^2 \theta_f^2)} + \frac{E_\gamma(1 + \bar{\gamma}^2 \theta_f^2)}{4\bar{\gamma}^2 E_p} \right] \right. \\ & \left. - \frac{\bar{\gamma}^2 \theta_f^2}{(1 + \bar{\gamma}^2 \theta_f^2)^2} \right\} \times \exp\left(-\frac{(\theta_x - x_c/L)^2}{2\sigma_{\theta_x}^2} - \frac{(\bar{\gamma} - \gamma_0)^2}{2\sigma_{\bar{\gamma}}^2}\right) d\theta_x dx_c dy_c \end{aligned}$$

The set energy of the electron beam is adjusted with an increment of 0.02 MeV. The relative increase is about 4×10^{-5} .

$$461.06 \rightarrow 461.08 \rightarrow 461.10 \rightarrow 461.12 \rightarrow 461.14 \text{ MeV}$$

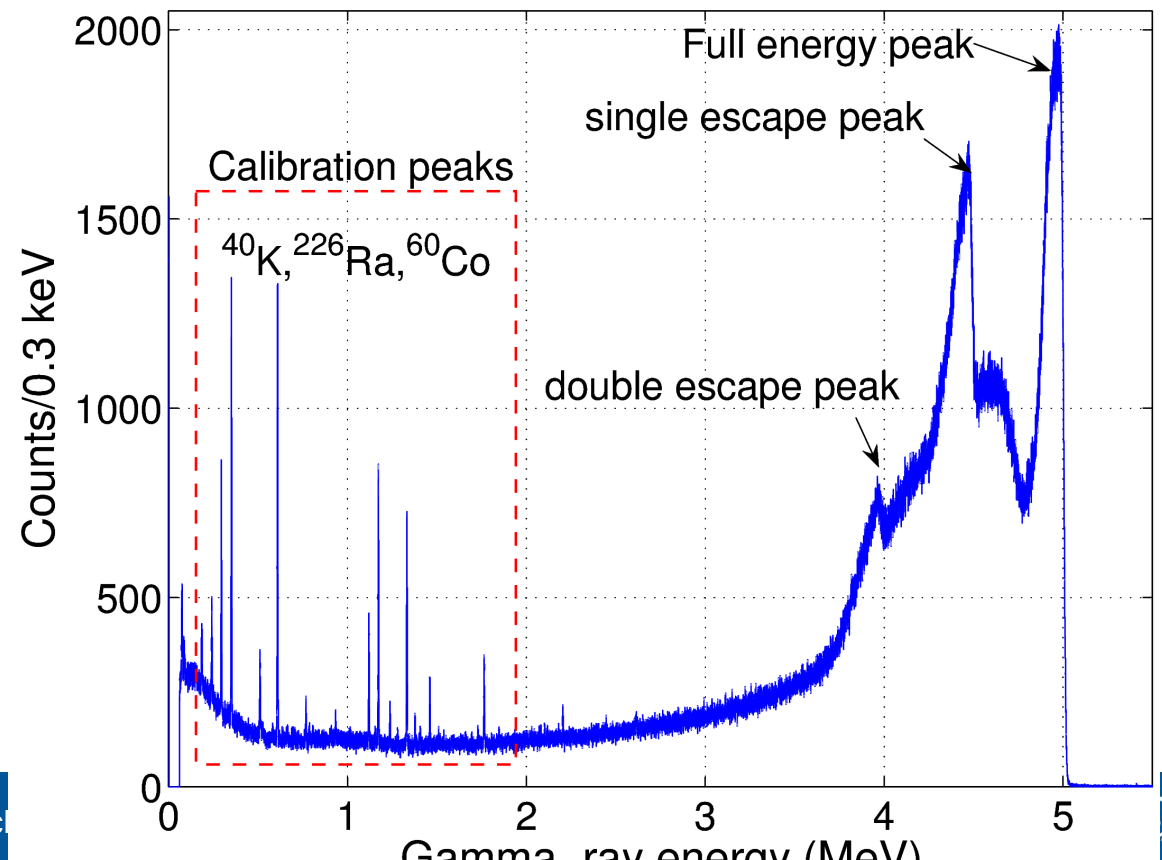


Measured Energy vs Set Energy



TAB. 1 – Uncertainty of the electron beam energy measurement at the storage ring set-energy of 461.06 MeV.

Error types	Gamma beam			FEL		
	δE_g (keV)	δE_e^i (MeV) ¹	$\delta E_e^i/E_e (\times 10^{-5})$	$\delta \lambda_{ph}$ (nm)	δE_e^i (MeV) ²	$\delta E_e^i/E_e (\times 10^{-5})$
Statistical	0.087	0.0040	0.87	0.0018	0.00052	0.11
Systematic	0.188	0.0087	1.9	0.032	0.0092	2.0



TAB. 1 – Uncertainty of the electron beam energy measurement at the storage ring set-energy of 461.06 MeV.

Error types	Gamma beam			FEL		
	δE_g (keV)	δE_e^i (MeV) ¹	$\delta E_e^i/E_e (\times 10^{-5})$	$\delta \lambda_{ph}$ (nm)	δE_e^i (MeV) ²	$\delta E_e^i/E_e (\times 10^{-5})$
Statistical	0.087	0.0040	0.87	0.0018	0.00052	0.11
Systematic	0.188	0.0087	1.9	0.032	0.0092	2.0

- The overall uncertainty of the measurement is about few 10^{-5} .
- This accuracy is comparable to another technique, Resonant Spin Depolarization.